Direct and indirect fitness effects of competition limit evolution of allelopathy in an invading plant

Richard Honor, Mia Marcellus[1], Robert I. Colautti*

Queen's University, 99 University Ave, Kingston, ON K7L 3N6

[1] Current Address: McGill University, 845 Sherbrooke St W, Montreal, QC H3A 0G4

*Corresponding author e-mail: robert.colautti@queensu.ca

Keywords: allelopathy, glucosinolates, biological invasions, trade-off, novel weapons hypothesis, rapid evolution

Abstract

1. Upon introduction to new continents, invading species encounter novel communities of consumers, pathogens, and competitors. Both phenotypic plasticity and rapid evolution can facilitate adaptation across these heterogenous communities, facilitating further invasion. However, the rate and extent of adaptive evolution on contemporary timescales can be constrained by phenotypic plasticity and limits imposed by genetic co-variation for traits under selection.
2. We measured phenotypic plasticity and quantified genetic co-variation for growth, competition, and fitness among 23 naturally inbred seed families of *Alliaria petiolata* (garlic mustard) collected across its invasive range in eastern North America. After growing a self-pollinated generation in a uniform common garden to reduce maternal effects, we reared second-generation plants in a two-year greenhouse and field experiment with naïve soil from an uninvaded habitat. We measured selection gradients and lifetime fitness when reared alone, with an intraspecific competitor, and under interspecific competition with naïve *Acer saccharum* (sugar maple) saplings.
3. Total glucosinolate production was strongly correlated with the production of chlorophyll *a* (Chl *a*) ($R^2 = 0.45$) such that first principal component (PC1) accounted for 84% of variation in these two traits. Furthermore, PC1 exhibited high plasticity across growing environments ($p < 0.001$) with limited broad-sense heritability ($H^2 = 2.91$; $p = 0.08$). In contrast, investment in glucosinolate production relative to Chl *a* (PC2) was significantly heritable ($H^2 = 16.91$, $p < 0.001$) with minimal plasticity across treatments. Causal analysis revealed that plastic variation for higher Chl *a* + glucosinolate production (PC1) had an indirect positive effect on *A. petiolata* fitness via a direct, negative effect on *A.*

43 *saccharum* performance. In contrast, heritable variation for higher glucosinolate
44 investment (PC2) had a direct, positive effect on *A. saccharum* performance and an
45 indirect negative effect on *A. petiolata* fitness.

46 4. *Synthesis.* Applying causal inference, we find that evolution of allelopathy in *A. petiolata*
47 has been constrained by (i) a lack of genetic variation, (ii) selection against glucosinolate
48 investment under interspecific competition, and (iii) phenotypic plasticity. These factors
49 limit adaptive evolution but maintain fitness during population growth as plants switch
50 from interspecific to intraspecific competition during invasion.

Introduction

Adaptive evolution over geological timescales should produce populations that are well-adapted to their local environment. Yet, a variety of invasive taxa spread to new geographic regions where they displace native species, despite having much less time to adapt to the new biotic and abiotic challenges they face. This phenomenon is sometimes called the 'paradox of invasion' (Sax and Brown 2011), which can be resolved through phenotypic plasticity and rapid evolution, each of which can help invasive species to thrive in variable environments. For decades, biologists have speculated about the importance of plasticity and adaptation to the spread of invasive species but the relative contribution of each remains an area of active research (Baker and Stebbins 1965; Parker et al. 2003; Richards et al. 2006; Barrett 2016).

There is growing evidence that rapid evolution can facilitate invasion, possibly by relaxing evolutionary constraints in the introduced range (reviewed in Colautti and Lau [2015]). For example, life history evolution in expanding populations has been shown to increase rates of spread in greenhouse and growth chamber experiments (Williams et al. 2016; Ochocki and Miller 2017; Szücs et al. 2017). In North America, the invasive perennial herb *Lythrum salicaria* (purple loosestrife) rapidly evolved to adapt to differences in season length along a latitudinal gradient, increasing reproductive fitness by an order of magnitude (Colautti and Barrett 2013). In Australia, *Rhinella marina* (cane toads) evolved morphological changes that increase dispersal at the invasion front, increasing the rate of spread (Philips et al. 2006; Shine et al. 2021). These examples demonstrate how evolution can occur rapidly in invasive species along abiotic environments and density gradients. However, less is known about the evolutionary response of invasive species to novel biotic interactions arising during invasion.

Several hypotheses attribute invasions to ecological and genetic differences between native and introduced regions, but experimental studies are often inconclusive. In particular, the loss of specialist herbivores in invading plant populations could favour the evolution of more competitive genotypes when costly defences are no longer needed (Blossey and Notzold 1995; Keane and Crawley 2002; Müller-Schärer et al. 2004; Doorduin and Vrieling 2011). In addition to defending against herbivory, some secondary metabolites can have allelopathic effects on competitors (Inderjit et al. 2008; Gomes et al. 2017; Hierro and Callaway 2021; Inderjit et al. 2021). Natural selection may favour higher concentrations of these metabolites in the introduced range where native competitors are relatively naïve, and thus more susceptible to their effects (Callaway and Ridenour 2004; Lankau et al. 2009). Hypotheses invoking an escape from specialist natural enemies or shifts in competitive interactions are not mutually exclusive; for example, a reduction in herbivory might lead to an evolutionary shift in chemistry from defensive to allelopathic (Uesugi and Kessler 2013). However, most of the experimental evidence supporting these hypotheses involves average differences in phenotype between continents (e.g., Europe and North America), yet biotic and abiotic factors are typically more variable at the scale of local populations. Indeed, there is good evidence that spatial autocorrelation and non-random sampling confound experimental comparisons of native and introduced populations (Colautti et al. 2009; Colautti and Lau 2015). Geographic isolation also reduces gene flow, facilitating post-introduction evolutionary divergence. As a result, both neutral markers and heritable trait variation are often more variable among populations within the introduced range than between ranges (Dlugosch and Parker 2008; Colautti and Lau 2015).

Despite growing evidence for rapid evolution within the introduced range, little is known about the biotic drivers of divergence among introduced populations.

The 'Chicago School' of ecological genetics defines an experimental approach to study trait evolution in natural populations by separately assessing natural selection and heritable genetic variation (Endler 1986; Conner and Hartl 2004). Under this framework, the strength and direction of natural selection is estimated by linear regression), and a multiple regression can quantify both direct selection on a single trait and indirect selection via selection on correlated traits (Lande and Arnold 1983. In addition to quantifying natural selection, genetic variation for traits under selection can be estimated as the proportion of trait variation explained by genetic relatedness among individuals. Both natural selection and heritable trait variation are necessary for adaptive evolution to occur, yet both factors are assessed concurrently to study evolution during invasion (Colautti and Lau 2015). For example, chlorophyll *a* (Chl *a*) and glucosinolate production are often linked via pleiotropy (Chen et al. 2012) and chromosomal linkage (Qian et al. 2016). Pleiotropy constrains short-term evolutionary changes such that evolution of glucosinolate production could occur via direct selection on glucosinolates or as an indirect response to direct selection on Chl *a*. Selection gradients and genetic variation jointly predict the rate and direction of adaptive evolution, but both are contingent on the environmental context in which they are measured.

Understanding evolution across continental to intercontinental scales requires careful consideration of the context-dependency of selection at the local population scale (Colautti & Lau 2015). For example, secondary metabolites in plants can have both direct effects on fitness

and indirect effects mediated through ecological interactions. These indirect ecological effects are not easily assessed using the Lande-Arnold multiple regression framework (Scheiner et al. 2000). Instead, structural equation models, path analysis, and other forms of causal analysis test hypotheses about natural selection acting through direct and indirect ecological mechanisms (Kingsolver and Schemske 1991; Scheiner et al. 2000; Shipley 2016). Causal inference can be particularly useful for investigating allelopathy and competition.

The biennial herb *Alliaria petiolata* (garlic mustard) is an emerging model system in ecological genetics (Alabi et al. 2021) with relevance to broader questions about the role of ecological interactions in the rapid evolution and spread of invasive species (Rodgers et al. 2022). A member of the mustard family (Brassicaceae), *A. petiolata* is native to Eurasia and invading forest understories of North America, where it can be an aggressive weed (Rodgers et al. 2008). Members of the Brassicaceae family produce glucosinolates for a variety of ecological purposes including defence against pathogens and herbivores, and tolerance to other environmental stresses (Holst and Fenwick 2003; Hopkins and Hüner 2009). Glucosinolates produced by *A. petiolata* enter the soil through shoot decomposition and root exudation (Barto and Cipollini 2009; Cantor et al. 2011), which can disrupt mycorrhizal communities and reduce mycorrhizal colonization of host plants (Roberts and Anderson 2001; Stinson et al. 2006; Callaway et al. 2008; Wolfe et al. 2008; Cantor et al. 2011). However, these indirect allelopathic effects are inconsistently observed, depending on experimental conditions and the presence of susceptible neighbours and mycorrhizae (Burke 2008; Barto et al. 2011; Burke et al. 2019; Duchesneau et al. 2021; Roche et al. 2021). Understanding the context dependency of glucosinolate-soil interactions remains an active area of research in this species.

142

143 Glucosinolate concentration in *A. petiolata* is a good candidate trait for investigating
144 environment-dependent, eco-evolutionary feedbacks involving allelopathic interactions because
145 invading populations shift from primarily interspecific competition to strong intraspecific
146 competition as populations grow (Lankau et al. 2009; Evans et al. 2016). Glucosinolate evolution
147 can be constrained by pleiotropy and chromosomal linkage with Chl *a* production and other
148 performance traits (Misyura et al. 2013; Qian et al. 2016), which would limit adaptive evolution.
149 Plasticity can also limit the evolutionary response to selection by masking heritable genetic
150 variation, and glucosinolates in *A. petiolata* is known to vary across competitive environments
151 (Cipollini 2002; Cipollini et al. 2005; Smith 2015). Understanding trait correlations, genetic
152 variation, and phenotypic plasticity across competitive environments is therefore crucial for
153 reconstructing the history of adaptive evolution during invasion and for predicting future
154 evolutionary trajectories.

155

156 Here, we test the hypothesis that introduced populations of *A. petiolata* evolved local differences
157 in glucosinolate investment as populations shifted from inter- to intra-specific competition
158 during invasion. Specifically, we address four main predictions. First, we ask how much genetic
159 variation exists for glucosinolate investment in *A. petiolata* genotypes sampled across eastern
160 North America. A lack of heritable genetic variation represents an evolutionary constraint.
161 Second, we assess plasticity in glucosinolate investment across competition treatments.
162 Phenotypic plasticity can simultaneously limit adaptive evolution while improving survival and
163 reproduction across heterogenous environments. Third, we ask whether natural selection reverses
164 from favouring higher glucosinolate investment under interspecific competition to favouring

lower investment under intraspecific competition and non-competition treatments, as this is a key fitness trade-off required for eco-evolutionary dynamics of glucosinolate production. Finally, we test whether glucosinolate investment increases fitness of *A. petiolata* indirectly via suppression of an interspecific competitor. This is important because the evolution of allelopathy requires a fitness benefit that is mediated indirectly through suppression of competition. To address these questions, we combine causal analysis with methods from the Chicago School to estimate direct and indirect selection, characterize genetic variation, and quantify phenotypic plasticity.

Materials and Methods

Study species

Alliaria petiolata (garlic mustard) is emerging as a model system for integrated studies in invasion biology (Kueffer et al. 2013; Colautti et al. 2014; Alabi et al. 2021). Native to much of Eurasia, it was first recorded in North America in 1868 in Long Island, New York (Rodgers 2008). Most densely populated along the East Coast of North America, *A. petiolata* is also found in the Prairies and along the West Coast between Alaska and Oregon (Anderson 2012). As an obligate biennial species, it emerges in early spring, overwinters as a rosette, and then forms a flowering bolt in the following spring (Cavers et al. 1979; Anderson et al. 1996; Cruden et al. 1996). *Alliaria petiolata* reproduces sexually and it is pollinated by a variety syrphid flies, midges and bees, yet over 80% of seeds are produced through self-fertilization and roughly 80% of the genetic variation for neutral markers is partitioned among populations, consistent with high selfing rates (Durka et al. 2005). Despite high selfing rates, the species does not tend to suffer from inbreeding depression, (Mullarkey et al. 2013) possibly due to its hexaploid genome, genetic purging, and periodic outcrossing.

188

189 *Acer saccharum* (sugar maple) is a shade tolerant tree that is native to over 25 different forest
190 types in North America; it typically grows in cool moist regions between the latitudes of
191 approximately 35° and 50° (Ralph 1998). Its seeds exhibit very high germination success (~95%)
192 and densities regularly exceed 37 saplings per m^2 in the forest understory (Godman et al. 1990).
193 The high sapling density and reliance on root mycorrhizal associations make *A. saccharum* a
194 primary competitor of *A. petiolata* and a good model for allelopathy studies (Stinson et al. 2006).
195 Early molecular work identified reduced root colonization by mycorrhizae where the two species
196 co-occur (Barto et al. 2011), though a detailed high-throughput sequencing study did not detect
197 an effect of *A. petiolata* on soil endomycorrhizal communities (Duchesneau et al. 2021).

198

199 **Seed sources**

200 *Alliaria petiolata* seeds were collected between 2009–2012 as part of the Global Garlic Mustard
201 Field Survey (Colautti et al. 2014) with methods detailed therein. Our experiment uses the
202 offspring of a single plant per population (i.e., "seed family") as a representative of the naturally
203 inbred parent population. Seed families are thought to adequately capture the genetic profile of
204 the parent population, because *A. petiolata* exhibits high inbreeding and populations harbor low
205 within-population genetic variation (Durka et al. 2005). To dilute maternal effects on growth and
206 fitness, seed families were first grown in an outdoor common garden at the Queen's University
207 Biological Station (QUBS; 44.5671° N, 76.3250° W) in 2017-2018. Four seed families were
208 additionally derived from the original field collection to increase the geographical scope of
209 samples (Figure 1; Table 1).

210

211 On May 8, 2019, we collected *Acer saccharum* saplings from a natural population located in a
212 forest understory adjacent to a gravel road near the common garden site at QUBS. This section
213 of the forest was not yet invaded, but it appeared to be suitable habitat as there was an expanding
214 *A. petiolata* population as near as 25 m. Blocks of soil, approximately 15cm deep with an
215 abundance of *A. saccharum* saplings, were transported back to the greenhouse where saplings
216 were placed into experimental pots. We retained soil around roots to avoid disrupting root hairs
217 and associated mycorrhizal connections. Additional field soil was collected from this area by
218 removing debris and other plant material from the surface of the soil, and then collecting the top
219 layer to a depth of ~ 12 cm. The soil was then thoroughly homogenized using shovels and rakes
220 prior to use in the glasshouse.
221
222 **Experimental design**
223 *Alliaria petiolata* seeds were stratified in the dark at 4°C in Parafilm™-sealed petri dishes
224 containing 2mL of deionized water and untreated field soil, to maintain characteristics and
225 microbiota of natural soil. We monitored germination from March 7–May 7, 2019. Seeds that did
226 not germinate by March 26, 2019, were forced to germinate using scarification and 2mL of
227 0.001M gibberellic acid, as per Sosnoskie and Cardina (2009).
228
229 Upon germination, we transferred seedlings into 2cm x 2cm plug trays filled with a 1:1 mixture
230 of sand and Sun Grow Sunshine® Mix #2 potting soil, which does not contain added nutrients.
231 Trays were watered as needed with deionized water to maintain soil saturation. To limit variation
232 in growth among seed families with different germination times, we maintained seedlings at a
233 constant 10°C (12h half daylight) in a growth chamber in the Queen's University Phytotron.

We transplanted all available seedlings on May 9–10, 2019, into 4-inch plastic pots (surface area = 81cm^2; volume = 524.39 cm^3) containing a 1:1 mixture of field soil and Sun Grow Sunshine® Mix #2 potting soil. Pots were moved to a glasshouse room in the Queen's University Phytotron, and we randomized the location of each pot across 5 tables. In the glasshouse, plants received natural light, filtered with a shade cloth to simulate a forest overstory, and were broadcast watered with a rubber hose once or twice per day as needed to maintain soil that was moist to the touch.

To determine the competitor pairs to be used in the intraspecific treatment, we wrote a short algorithm in R to randomly pair individuals from different seed families without repeating pair combinations. To limit human error in labelling and data collection, we used the baRcodeR package in R to generate a unique, scannable 2-dimensional barcode for each plant (Wu et al. 2020). The effective total sample size was 365 *A. petiolata* plants, with a median of 16 plants per seed family. However, sample size varied across 23 families due to variation in germination, survival, and sample loss associated with glucosinolate and Chl *a* processing (Table 1).

Starting with 23 genetically distinct *A. petiolata* accessions from the Global Garlic Mustard Field Survey (Colautti et al. 2014), we grew at least 3 individuals from each accession in each of 3 different competitive environments: (i) alone, (ii) interspecific competition with *A. saccharum*, and (iii) intraspecific competition with a different *A. petiolata* seed family (Table 1; Figure A1). We also grew 31 *A. saccharum* seedlings alone (i.e., the "maple alone" treatment), as a control for comparison with *A. saccharum* growth and survival in the interspecific treatment. In natural

conditions, *A. petiolata* density can be as many as 18 plants/dm^2 in April and dwindle to as little as 0.6 plants/dm^2 by June (Anderson et al. 1996). In comparison, density in our experiment was either 1.23 plants/dm^2 in the alone treatment or 2.46 plants/dm^2 in the intraspecific treatment.

In the first growing season, these plants grew in pots at the Queen's University Phytotron to limit environmental influences on leaf chemistry traits, growth rate, and total leaf area. *Alliaria petiolata* is a biennial herb that requires an overwinter vernalization period to promote flowering (Cavers et al. 1979). Therefore, plants were transplanted from the glasshouse into a field site (QUBS, 44.56 °N, 76.32 °W) at the end of the first growing season, to allow plants to acclimatize to cold temperatures before winter. This not only promoted flowering of *A. petiolata*, but additionally allowed us to assess overwinter survival and lifetime fecundity under natural field conditions.

Field common garden

On October 5, 2019, we transported all surviving plants from the greenhouse into a field plot at the QUBS field site, which included 2 m tall aluminum fencing to exclude vertebrate herbivores. We allowed plants to acclimate to colder temperatures by transplanting all plants in the fall, on October 5, 2019. To limit interactions with surrounding vegetation, we buried pots directly into the field soil, arranged into 49 experimental blocks with dimensions 0.6 m × 1.2 m and 15 cm deep, with pots spaced 10 cm apart.

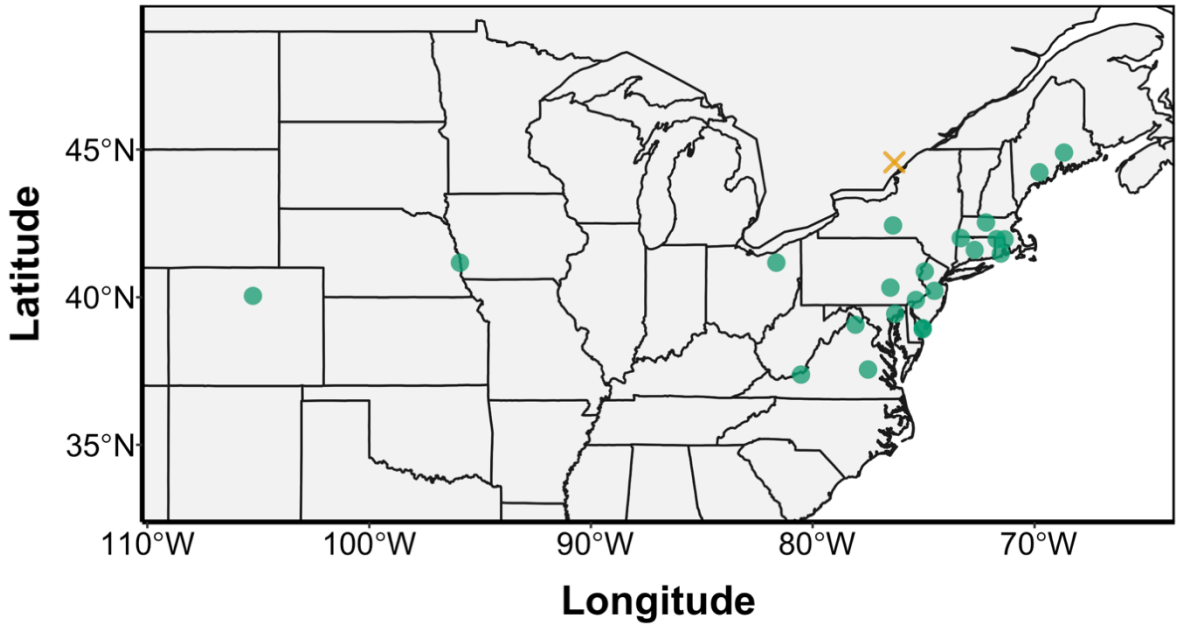

Figure 1. Sampling locations of naturally inbred seed families used in the experiment (green dots) excluding one family (EFCC2-4-80), which was sampled from northern Italy. The yellow "X" indicates the location of the field common garden site at the Queen's University Biological Station (QUBS), and where *Acer saccharum* seedlings were collected.

Table 1. Summary of seed sampling locations and number of surviving individuals from each accession in each of three treatments: alone, intraspecific competition, and interspecific competition.

Accession	Lat	Long	Alt (m)	N Alone	N Intra	N Inter
JBCHY1-1-50	38.95	-75.05	25.9	8	9	9
JBBLB2-1-20	38.91	-75.05	0	7	7	8
CRSOSO-3-40	44.9	-68.68	59	8	6	7
SMITH1-20	42.43	-76.39	326	4	9	8
CWRIC2-X2	37.54	-77.51	30	8	5	7
DVGM-20	40.88	-74.96	232	7	5	8
KVEDG1-1-80	39.44	-76.29	2	6	8	6
MHBUR1-4-20	41.97	-71.71	128	8	5	7
WSSWM3-1-0	39.91	-75.36	23	6	5	9
JWBOY-2-80	39.06	-78.07	250.9	7	6	5
MAVBEL2-1-20*	41.17	-95.9	358	5	6	6
VRCAN-1-40	42	-73.33	203	6	4	6
VRPET2-3-20	42.53	-72.19	329.1	8	4	4
BWPEM1-9-0	37.37	-80.52	1156	4	6	5
EFCC2-4-80	45.7	11.69	73	4	4	5
JARI1-1-80	41.48	-71.52	20.7	5	5	3
SMAKC1-B*	41.17	-81.64	307	4	4	5
VSGARO1-1-0	44.23	-69.78	62	5	3	5
MSMID1-1-20	41.6	-72.7	5	4	2	4
CBMCK1-1-0*	40.04	-105.23	1606.9	4	4	1
PDVRT1-20	40.22	-74.52	52	3	4	2
MHNAT1-2-0	41.96	-71.35	60	2	2	3
RULEB1-20*	40.33	-76.51	146.3	2	3	1
Total				**125**	**116**	**124**

*Seed families were derived from the original field collection

Greenhouse measurements (year 1)

To account for variation in time to germination and seedling size at transplant, we measured the length of the largest leaf and the number of true leaves on *A. petiolata* on May 16 and 17, 2019. To account for variation in *A. saccharum* size at transplant, we measured stem height, the number of true leaves and the length of the largest leaf on *A. saccharum*. At the end of the first growing period in the glasshouse (August 14 to 21, 2019), we estimated total leaf area (TLA) on both plants as the leaf length multiplied by leaf width, summed across all leaves (hereafter TLA_{AS} for *A. saccharum* and TLA_{AP} for *A. petiolata*).

Growth rates of *A. petiolata* were calculated from rosette growth in bi-weekly measurements. Rosette size at each two-week census was measured by analyzing top and lateral images of each plant. As detailed in Appendix A of the Supporting Information, we used a machine learning algorithm in Python with packages OpenCV2 and PlantCV to identify pixels corresponding to leaves, and then to count the number of leaf pixels as an relative measure of rosette size (Bradski 2000; Python Core Team 2015; Berry et al. 2018). These estimates were validated by hand-measurements (see Supporting Information Appendix A). Plants were imaged every two weeks over the course of two days, but most growth occurred between the first (May 27 and 28) and second (June 11 and 12) censuses. We calculated relative growth rate between these two time periods:

$$\text{Relative growth rate} = \frac{\ln(Rosette\ size_2) - \ln(Rosette\ size_1)}{t_2 - t_1} \qquad 1$$

where t denotes the time in seconds (Unix time), and subscripts indicate the census.

322 **Leaf chemistry**

323 To quantify glucosinolate and Chl *a* concentration in *A. petiolata*, we sampled leaf tissue at the
324 end of the first growing season (August 14 to 21, 2019). Two leaf punches of 8 mm diameter
325 from a single leaf were immediately placed in an Eppendorf® 1.5mL flip-cap tube and flash-
326 frozen in liquid N_2 prior to storing at -80 °C. Up to two leaves were sampled per plant, and the
327 two smallest leaves that were greater than 30 mm in length were chosen for sampling from each
328 plant. We excluded leaves with more than 50% senescence and/or pathogen damage. Leaf area
329 (length × width) was also recorded for each leaf sampled, hereafter referred to as leaf area of the
330 sampled leaf, to account for dilution effects associated with leaf cell expansion (Cipollini and
331 Gruner 2007).

332

333 Leaf tissue was kept frozen and pulverized using two cycles of 15 seconds using a Next Advance
334 Bullet Blender® at maximum speed (6 kHz). We submerged in liquid N_2 between cycles to limit
335 thawing of the plant tissue. After pulverization, we added 0.55 mL of 100 % methanol and
336 incubated in an Eppendorf Mixmate Vortex shaker for 1 hour at 25 °C and 300 rpm, followed by
337 centrifugation for 2 minutes at 2500 g (Eppendorf, 5427 R). Two 20 µL extracts of supernatant
338 were evaporated and resuspended in 50µL of 100% methanol. Then, Chl *a* concentration was
339 quantified with UV spectroscopy following Ritchie (2006):

340

341 $$\text{Chl } a \left(\frac{\mu\text{g}}{\text{ml}}\right) = -8.0962(A_{652} - A_{750}) + 16.5169(A_{665} - A_{750}) \quad 2$$

342

343 where *A* is the absorbance and subscripts denote the wavelength in nanometers (nm).

344

345 From the remaining supernatant, 465 µL was rinsed with 650 µL of hexane to remove
346 hydrophobic pigments that overlap the target wavelength (Haribal and Renwick 2001; Callaway
347 et al. 2008). Samples were centrifuged at 2500 g for 10 minutes at 4 °C. Glucosinolate
348 concentration of the supernatant was quantified with UV spectroscopy following methods in
349 Ishida et al. (2011) and Ishida et al. (2012), which we modified by using 100 µL of 3.5 mM
350 sodium tetrachloropalladate ($NaCl_4Pd$) instead of 3 mL of 2 mM $NaCl_4Pd$, to enable assays in a
351 96-well plate (Mawlong et al. 2017). Known concentrations (0.0625, 0.1250, 0.2500, 0.5000, and
352 1.0000 mg/ml) of sinigrin were used as a standard as it is one of the most abundant
353 glucosinolates in *A. petiolata* and is suspected to have allelopathic effects (Vaughn and Berhow
354 1999). The assays were read at 425 nm before and after adding an equal volume of $NaCl_4Pd$.
355 This diluted the second sample by half; therefore, we divided the first reading by 2 and
356 subtracted from the second reading to estimate total glucosinolate concentration:
357

358 $$\text{Total glucosinolate (mg/ml)} = 0.69\left(A_2 - \frac{A_1}{2}\right) - 0.15 \qquad 3$$

359

360 Where A is the absorbance at 425 nm and subscripts denote before (A_1) and after $NaCl_4Pd$ was
361 added (A_2). Glucosinolate concentration was estimated from a standard curve of sinigrin
362 (Supporting Information Figure A3).
363

364 As a more stringent quality control, we extracted glucosinolates from *A. petiolata* leaf material to
365 generate a standard sample to use as a control in every 96-well assay we performed. If the
366 glucosinolate concentration of the standard sample in any 96-well plate assays was more than 2.5
367 standard deviations from the mean glucosinolate concentration of the standard sample, the entire

368 96-well plate assay was discarded. Some samples were also lost due to cracking in the flip-cap
369 tube during processing, or were excluded from sampling because they had observable pathogen
370 damage or leaf senescence. Of the 506 plants in the experiment, 267 plants had samples from
371 two leaves, 98 plants had samples from one leaf, and 141 plants had no samples. Glucosinolate
372 and Chl *a* were averaged in plants with samples from two leaves for analyses.
373
374 **Biotic interactions**
375 By using non-sterile field soil, we exposed plants to naturally occurring pathogens and
376 germination of spores and small seeds present in the soil, which were primarily represented by
377 *Sphagnum* moss, which covered the soil surface, and ferns from the family Dryopteridaceae,
378 which colonized sporadically. On October 1, 2019, the number of ferns in each pot were counted
379 to a maximum of 15 individual plants to use as a covariate in our analysis. On *A. petiolata*
380 leaves, we observed thrips (order Thysanoptera), a powdery mildew fungus identified as
381 *Erysiphe cruciferarum*, and black rot (*Xanthomonas campestris*). These pathogens commonly
382 infect the Brassicaceae (Ciola and Cipollini 2011; Vicente and Holub 2013), and were identified
383 based on the characteristics of leaf lesions (see Supporting Information Figure A2 for examples).
384
385 Enemy abundance was evaluated by photographing the same leaves that were chosen for
386 glucosinolate and Chl *a* quantification. On each leaf, thrip damage and *X. campestris* lesions
387 were counted, and the presence of *E. cruciferarum* was recorded (Figure A2). *Acer saccharum*
388 also exhibited leaf damage, observable as leaf holes likely of thrip origin, which were small but
389 still visible to the naked eye. The presence of leaf damage on each leaf was recorded while

390 TLA_{AS} was measured, and the proportion of damaged *A. saccharum* leaves on each plant was
391 used to indicate pathogen damage for that species.
392
393 **Field measurements (year 2)**
394 On May 13, 2020, we recorded overwinter survivorship. At the end of year 2 (July 8 to 9, 2020),
395 siliques from all remaining *A. petiolata* plants, and the shoots of all remaining *A. saccharum*
396 plants were harvested at the soil base. Plant material was then dried to constant weight before
397 measuring dry biomass. Additionally, we separately measured silique biomass as our estimate of
398 reproductive fitness in *A. petiolata*, whereas shoot biomass was our estimate of performance of
399 *A. saccharum*. As a biennial, lifetime fitness of *A. petiolata* was calculated as the joint
400 distribution of survival and silique biomass at the end of the experiment, including plants that did
401 not survive to reproduce (lifetime fitness = 0).
402
403 **Principal components analysis**
404 Multicollinearity in regression analysis can produce unreliable p-values and coefficients with
405 large standard errors (Crawley 2007). As noted in the introduction, Glucosinolates and Chl *a* are
406 often correlated due to chromosomal linkage and pleiotropy, which can compromise estimates of
407 natural selection. Therefore, we conducted a principal component analysis (PCA) to define
408 biologically meaningful axes of variation while avoiding the problem of multicollinearity,
409 following Colautti and Barrett (2011). We also quantified the extent of plasticity and genetic
410 variation along both principal component axes, as described in the next section.
411

412 In addition to the PCA on Chl *a* and total glucosinolates, we ran two other PCAs to summarize
413 the transplant size measurements of *A. saccharum* (TS_{AS}) and *A. petiolata* (TS_{AP}). The TS_{AS}
414 PCA included stem height, largest leaf length and number of leaves, all measured after
415 transplant, as well as stem height, number of leaves and TLA_{AS}, all measured at the end of year 1
416 (Supporting Information Table B1). The TS_{AP} PCA included initial largest leaf length and
417 number of true leaves, measured at transplant (Table B2). The first principal component of each
418 PCA were used in our statistical models, as described below.
419
420 **Estimating genetic variance and plasticity**
421 Statistical mixed models were used for each *A. petiolata* trait to estimate the proportion of total
422 phenotypic variation explained by genetic variation (G) among inbred seed families, plasticity
423 due to environmental (E) variation across competition treatments, and genetic variation for
424 plasticity (G × E) as the statistical interaction term. Each model took the form of a variance
425 partition analysis (Lynch and Walsh 1998; Crawley 2007) with each *A. petiolata* trait as a
426 dependent variable in a model with seed family and a family-by-treatment interaction as random
427 effects.
428
429 Mixed effects models were fit using the package glmmTMB in R (Brooks et al. 2017; R Core
430 Team 2020) and the significance of each effect was assessed using a likelihood ratio test (LRT).
431 Greenhouse bench and position within the field common garden were included only when
432 significant as determined by LRT, and we included leaf area as a covariate in models of leaf
433 chemistry traits. Reproducible R code for all statistical models is available through Dryad (doi:
434 XXX).

435

436 **Multivariate selection analysis of *Alliaria petiolata***

437 We measured selection using standardized selection gradients, which are partial regression
438 coefficients estimating the change in mean fitness in response to units of standard deviation of a
439 trait (Lande and Arnold 1983; Matsumura et al. 2012). Therefore, we first standardized fitness by
440 dividing each individual fitness value by the mean, and we standardized traits for selection
441 analysis to a mean of zero and standard deviation of one.

442

443 Mixed effects models were fitted to four separate models with TLA_{AP}, survival, fecundity, and
444 lifetime fitness, each as a response variable. In each case, the full model included an interaction
445 term for PC1 (i.e., general glucosinolate and Chl *a* production) and treatment, and a second
446 interaction term between relative glucosinolate investment (PC2) and treatment. These two-way
447 interactions represent a statistical test of whether the slope of direct selection on PC1 and PC2
448 differ across competition treatments. Our statistical models also included the fixed effects of
449 bench, fern abundance, TS_{AP}, relative growth rate, thrip damage, *X. campestris* infection, and *E.*
450 *cruciferarum* presence. The random effect of seed family was also included in all maximum
451 models. Fitness measured in the field common garden also included TLA_{AP} as a fixed effect
452 (covariate) and the random effects of row and column describing the spatial location of each
453 individual. A model of best fit for each fitness measurement was determined by sequentially
454 performing likelihood ratio tests of hierarchical models derived from the full model outlined
455 above.

456

457 Fecundity, lifetime fitness, fern abundance, thrip damage, *X. campestris* infection, glucosinolate
458 concentration, and Chl *a* concentration were each log-transformed to meet assumptions of
459 normality. If PC1 or PC2 was a significant predictor, the model was reassessed after controlling
460 for leaf area of the sampled leaf, because plant metabolites are most concentrated in younger,
461 smaller leaves, making PC1 and PC2 potentially autocorrelated with performance and fitness
462 (Cipollini and Gruner 2007). When family was a significant predictor, a separate model
463 excluding family was used when we wanted to include effects of heritable genetic variation.
464
465 A generalized linear model with a binomial error distribution and a logit link was used for model
466 selection of survival rates. Minimum adequate models were then converted to standardized
467 selection gradients after all terms were assessed for significance. Standardized selection
468 gradients of survival data were obtained by dividing data by the mean survival rate and fitting the
469 model with a gaussian error distribution (Hajduk et al. 2020). We did this because the predicted
470 response to selection is proportional to the additive genetic covariance between a trait and
471 fitness.
472
473 Selection gradients measure direct selection on a trait while controlling for selection on
474 correlated traits. To predict the change in mean trait value from one generation to the next, we
475 measured selection differentials for PC1 and PC2 in each treatment by subtracting the
476 phenotypic mean of all individuals from the phenotypic mean of individuals that survived; this
477 estimated change in mean phenotype includes the effects of direct selection on the trait and
478 indirect selection on correlated traits.
479

480 **Multivariate selection analysis of *Acer saccharum* performance**

481 As with *A. petiolata*, we used model selection with likelihood ratio tests of nested models to
482 assess the significance of interspecific competition on TLA_{AS} in year 1 and on the log-
483 transformed *A. saccharum* shoot biomass in year two (to meet normality assumptions). To assess
484 the average effect of interspecific competition on *A. saccharum*, the fixed effects of TS_{AS}, fern
485 abundance, bench, leaf damage and treatment (i.e., *A. saccharum* alone vs interspecific
486 competition treatment) were included in our statistical models.

487

488 To test whether glucosinolate production or unmeasured *A. petiolata* traits might affect *A.*
489 *saccharum* performance, we again used model selection with likelihood ratio tests on *A.*
490 *saccharum* performance in year 1 and 2. Fixed effects included TS_{AS}, leaf damage and fern
491 abundance, as well as the *A. petiolata* traits: relative growth rate, TLA_{AP}, PC1, PC2, and seed
492 family. Random effects included greenhouse bench, as well as field row and column in the year 2
493 model.

494

495 **Path analysis of indirect effects**

496 As with selection gradients, path coefficients are analogous to partial regression coefficients but
497 the latter can measure selection on a trait through hypothesized causal relationships (Scheiner et
498 al. 2000). We used standardized path gradients to measure direct selection on glucosinolate
499 production (PC1 and PC2) resulting from the allelopathic effect of glucosinolates on *A.*
500 *saccharum.* Four hypothetical path scenarios were analyzed, one for each *A. petiolata*
501 performance/fitness measure as the response, namely TLA_{AP}, survival, fecundity, and lifetime
502 fitness. Each path scenario included the direct effects of PC1 and PC2 on *A. petiolata*

503 performance/fitness, and the indirect effects of PC1 and PC2 on *A. petiolata* performance/fitness
504 via impacts on *A. saccharum* performance in year 1. We also included the significant predictors
505 of *A. saccharum* and *A. petiolata* performance in each. Greenhouse bench, field row and column
506 were not included in path analyses, as path analysis cannot handle categorical variables.
507
508 We used the Lavaan package (Rosseel 2012) for each path analysis, using permutation tests with
509 10,000 iterations to test for model significance. Each permutation test involved resampling either
510 PC1, PC2 or *A. saccharum* performance, refitting the model with these data, extracting the test
511 statistic, z, and taking its absolute value to generate a sampling distribution of z. The proportion
512 of random z-values greater than the true z-value gave the p-value ($\alpha = 0.05$). Separate tests were
513 performed for the effect of *A. saccharum* performance on *A. petiolata* fitness, the direct effects of
514 PC1 and PC2 on *A. petiolata* fitness, and the indirect effects of PC1 and PC2 on *A. petiolata*
515 fitness through *A. saccharum* performance.
516

517 **Results**

518 Mortality in the greenhouse (year 1) was 2.29 % for *A. petiolata* and 1.53 % for *A. saccharum*
519 but increased under field conditions (year 2) to 69.66 % for *A. petiolata* and 6.25 % for *A.*
520 *saccharum*. Total leaf area of *A. petiolata* (TLA_{AP}), fecundity, and lifetime fitness were lowest in
521 the intraspecific treatment (Supporting Information Table B3). For example, mean fecundity was
522 3.13 g (95 % CI = ± 0.84 g) in the alone treatment, 1.78 g (95 % CI = ± 0.83 g) in the
523 interspecific treatment and 1.07 g (95 % CI = ± 0.38 g) in the intraspecific treatment. In contrast,
524 *A. petiolata* mortality was highest in the interspecific treatment (73.62 %) compared to 68.18 %

525 (120/176) in the intraspecific treatment, and 65.27 % (109/167) in the alone treatment (Table
526 B3).
527
528 **Principal component analysis**
529 Consistent with studies of other species, we found that glucosinolate and Chl *a* production were
530 strongly correlated ($r^2 = 0.43$, $p < 0.001$). In the PCA of glucosinolate and Chl *a* production, PC1
531 accounted for 84% of the variation in these two traits, whereas PC2 accounted for 16 % (Figure
532 2, Supporting Information Table B4). Higher PC1 values represent individuals with greater leaf
533 tissue concentrations of both glucosinolates and Chl *a*. We therefore refer to PC1 as total
534 metabolite production. In contrast, higher PC2 values represent individuals with a higher
535 production of glucosinolates relative to Chl *a*, which we refer to as relative glucosinolate
536 investment. Mean PC1 was greatest in the alone treatment (0.47; 95 % CI = ±0.19), followed by
537 the intraspecific treatment (–0.05; 95 % CI = ±0.26), and the interspecific treatment (–0.43; 95 %
538 CI = ±0.21), while PC2 was similar across treatments (Supporting Information Table B3).
539

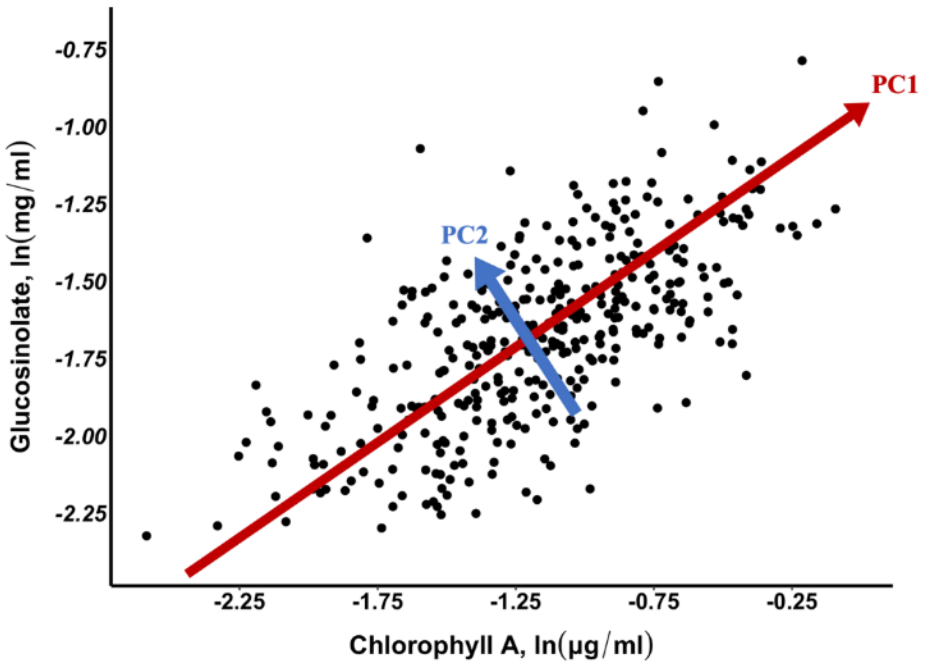

Figure 2. Bivariate plot of glucosinolate and Chl *a* production with approximate principal component eigenvectors PC1 (red) and PC2 (blue). The first principal component (PC1) represents total metabolite production and accounts for 84 % of the total variation in these traits. The second principal component (PC2) represents relative investment in glucosinolate production and accounted for 16% of the total variation. Higher PC2 values reflect greater production of glucosinolates relative to Chl *a*.

Plasticity and genetic variation

We found significant genetic variation amongst the 23 *A. petiolata* seed families for survival, transplant size (TS_{AP}), lifetime fitness, glucosinolate production, and PC2 (Table 2). Seed family explained 28.59 % of the variation in TS_{AP}, 17.96 % of the variation in survival and 7.38 % of the variation in lifetime fitness (all $p < 0.001$). Notably, seed family only explained 7.47 % of variation in glucosinolate production, and it was not a significant predictor of PC1 ($p = 0.08$) or

554 Chl *a* production ($p = 0.19$). In contrast, the effect of seed family on PC2 was highly significant
555 ($P < 0.001$) and explained 16.91 % of the phenotypic variance. Of the traits with detectable
556 genetic variation, only glucosinolate production and lifetime fitness varied significantly among
557 treatments. Transplant size (TS_{AP}) was a significant predictor of relative growth rate, total leaf
558 area (TLA_{AP}) and fecundity, but had little effect on the magnitude of variance estimates
559 (Supporting Information Table B5). Genetic variation was not detectable in the remaining traits,
560 which all exhibited strong plastic responses to treatment. We did not detect significant genetic
561 variation for plasticity in any traits in the form of statistical interactions between seed family by
562 competition treatment (Table 2).
563
564
565
566
567
568
569
570
571
572
573
574
575
576

577

578

579 **Table 2.** Percent of total phenotypic variation explained by family (broad sense heritability

580 [H^2]), treatment (plasticity) and a family-by-treatment interaction (genetic variation in

581 plasticity/reaction norms).

Variables	**Family (H^2)**	**Treatment**	**Family × Treatment**
	% (χ^2, p)	% (χ^2, p)	% (χ^2, p)
Transplant size	**28.59 (107.5, < 0.001)**	0.13 (0.3, 0.56)	2.57 (1.4, 0.24)
Chl *a**†	2.21 (1.7, 0.19)	**8.54 (27.1, < 0.001)**	< 0.1 (0, 1)
Glucosinolate*†	**7.47 (14.0, < 0.001)**	**8.78 (26.3, < 0.001)**	3.02 (0.6, 0.43)
Total metabolite production (PC1) †	2.91 (3.1, 0.08)	**10.95 (32.5, < 0.001)**	2.13 (0.3, 0.59)
Relative glucosinolate investment (PC2)	**16.91 (39.6, < 0.001)**	< 0.1 (0, 1)	<0.1 (0.1, 0.1)
Relative growth rate	1.89 (3.2, 0.07)	**11.19 (48.9, < 0.001)**	3.22 (1.3, 0.25)
TLA	0.17 (0.9, 0.35)	**27.40 (141.0, < 0.001)**	2.85 (1.8, 0.19)
Survival	**17.96 (22.3, < 0.001)**	0.26 (0.1, 0.79)	< 0.1 (0, 1)
Bolt size	<0.1 (0, 1)	**14.46 (17.1, < 0.001)**	< 0.1 (0, 1)
Fecundity*	< 0.1 (0, 1)	**11.52 (12.0, < 0.001)**	< 0.1 (0, 1)
Lifetime Fitness*	**7.38 (14.2, < 0.001)**	**3.51 (11.7, < 0.001)**	1.44 (0, 1)

582 Bold indicates $p < 0.05$

583 * Analyzed on log scale

584 † Leaf area of the sampled leaf included as a fixed effect.

585

586

Effect of *Alliaria petiolata* on *Acer saccharum* performance

When assessing treatment effects, TLA_{AS} in year 1 was best predicted by TS_{AS} ($\beta = +0.39$, $p < 0.001$), fern abundance ($\beta = -0.07$, $p < 0.05$), *A. saccharum* leaf damage ($\beta = -0.13$, $p < 0.001$) and treatment ($\chi^2 = 17.5$, $p < 0.001$). Compared to the alone treatment, interspecific competition reduced TLA_{AS} by –12.6% on average ($p < 0.001$). In the second year, *A. saccharum* shoot mass was best explained by treatment ($\chi^2 = 17.6$, $p < 0.001$) and TS_{AS} only ($\beta = +0.12$, $p < 0.001$). Interspecific competition reduced *A. saccharum* shoot mass in year 2 by –40.4% on average ($p < 0.001$).

When assessing which *A. petiolata* traits affected *A. saccharum*, TLA_{AS} was best explained by TS_{AS} ($\beta = +0.40$, $p < 0.001$), *A. saccharum* leaf damage ($\beta = -0.11$, $p < 0.001$) and the two *A. petiolata* traits, PC1 and PC2. While PC1 was negatively associated with TLA_{AS} ($\beta = -0.11$, $p < 0.001$), PC2 was positively associated with TLA_{AS} ($\beta = +0.07$, $p < 0.05$) (Figure 3). Shoot mass in year two was best explained by TS_{AS} ($\beta = +0.18$, $p < 0.001$), field row ($\chi^2 = 5.5$, $p < 0.05$), and the competitor trait, TLA_{AP} ($\beta = -0.13$, $p < 0.001$) (see Table B6 for all *A. saccharum* model selection results).

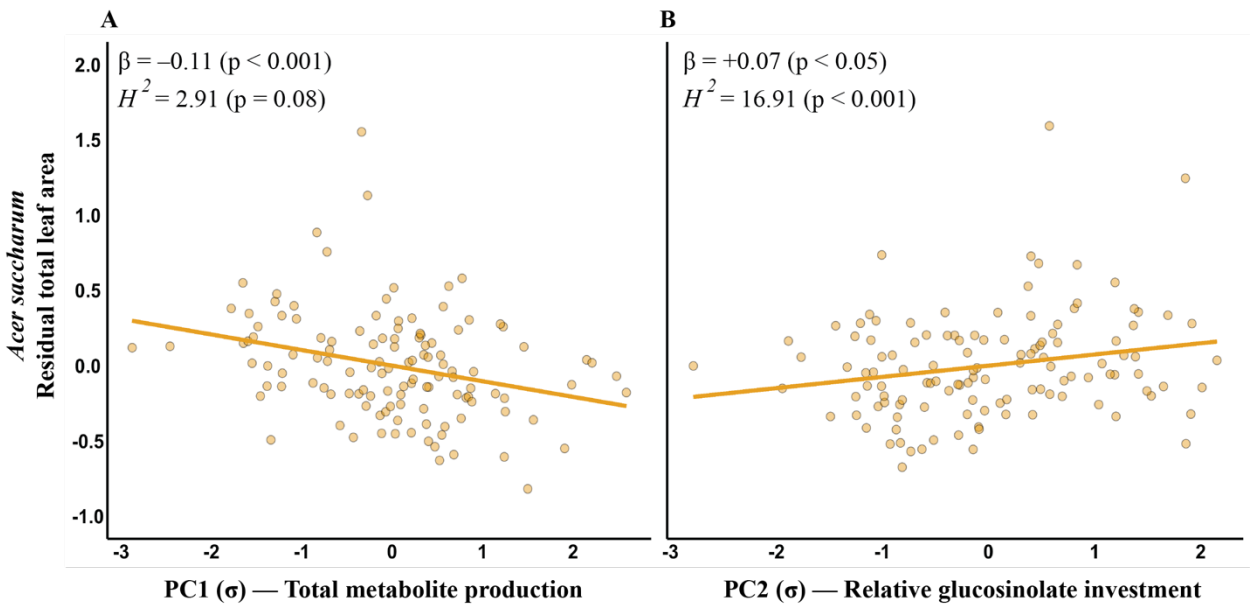

Figure 3. Effect of PC1 and PC2 on *Acer saccharum* total leaf area at the end of year 1. The y-axis shows the mean-standardized total leaf area (unitless) after controlling for *A. saccharum* transplant size and leaf damage. The x-axes show competitor *A. petiolata* PC1, representing the production of both glucosinolates and Chl *a* (panel A)*;* and PC2, representing investment in glucosinolates relative to Chl *a* (panel B). Both PC1 and PC2 were z-standardized to a mean of zero and unit standard deviation. The top left of each panel shows the regression coefficient (*β*) and the broad sense heritability (H^2) of PC1 (panel A) and PC2 (panel B).

Selection on *Alliaria petiolata* traits across treatments

Alliaria petiolata performance in year 1 (TLA_{AP}) was best explained by TS_{AP} ($\beta = +0.06$, $p < 0.001$), treatment, PC1, *X. campestris* infection ($\beta = -0.09$, $p < 0.001$), fern abundance ($\beta = -0.05$, $p < 0.01$) and the random effect of greenhouse bench ($\chi^2 = 29.9$, $p < 0.001$). We found a significant interaction between PC1 and treatment ($\chi^2 = 11.9$, $p < 0.01$), indicating different slopes. Specifically, PC1 was positively associated with TLA_{AP} in the interspecific treatment ($\beta = +0.10$, $p < 0.001$), but was not associated with TLA_{AP} in any other treatment (Figure 4). The

interaction between PC1 and treatment remained significant after controlling for leaf area of the sampled leaf ($\chi^2 = 12.6$, $p < 0.01$). Compared to the alone treatment, interspecific competition reduced TLA_{AP} by –15% ($p < 0.01$) while intraspecific competition reduced TLA_{AP} on average by –54% ($p < 0.001$).

Alliaria petiolata survival was best explained by fern abundance ($\beta = +0.35$, $p < 0.001$) and the random effects of family ($\chi^2 = 12.3$, $p < 0.001$) and field row ($\chi^2 = 6.7$, $p < 0.05$). The PC1 by treatment interaction was significant ($\chi^2 = 6.6$, $p < 0.05$), such that PC1 was positively associated with survival in the intraspecific treatment only ($\beta = +0.49$, $p < 0.05$). However, after accounting for leaf area of the sampled leaf, the effect was no longer significant ($\chi^2 = 5.3$, $p = 0.07$). When family was removed from the model, the effect of PC2 on survival was on the verge of significance ($\beta = -0.14$, $p = 0.059$). Interspecific competition reduced *A. petiolata* survival by –33% ($\chi^2 = 5.3$, $p < 0.05$). In contrast intraspecific competition was associated with a –7% reduction in *A. petiolata* survival, but was not significant ($p = 0.67$).

Selection differentials of survival were obtained by determining the mean change in trait value between surviving individuals (after purging selection) and all individuals (before purging selection). After selection, mean PC1 increased by +0.10 σ and +0.43 σ in the inter- and intra-specific treatments, respectively, but remained relatively constant in the *A. petiolata* alone treatment (–0.03 σ). In contrast, PC2 decreased by –0.22 σ and –0.32 σ in the inter- and intra-specific treatments, respectively, and remained relatively constant in the *A. petiolata* alone treatment (+0.01 σ).

Fecundity was best explained by TS_{AP} ($\beta = +0.24$, $p < 0.001$), PC1, and treatment ($\chi^2 = 9.4$, $p < 0.01$). Unlike in models of TLA_{AP} and survival, PC1 was positively associated with fecundity in all treatments ($\beta = +0.14$, $p < 0.05$) (Figure 4). Compared to the alone treatment, interspecific competition reduced fecundity by –50% ($p < 0.01$), while intraspecific competition reduced fecundity by –120% ($p < 0.001$) on average. Lifetime fitness was best explained by treatment ($\chi^2 = 15.5$, $p < 0.001$), family ($\chi^2 = 13.2$, $p < 0.001$) and field row ($\chi^2 = 9.0$, $p < 0.01$). Interspecific competition reduced lifetime fitness by –106% ($p < 0.001$), while intraspecific competition reduced lifetime fitness by –119% ($p < 0.001$; see Table B7 for all *A. petiolata* model selection results).

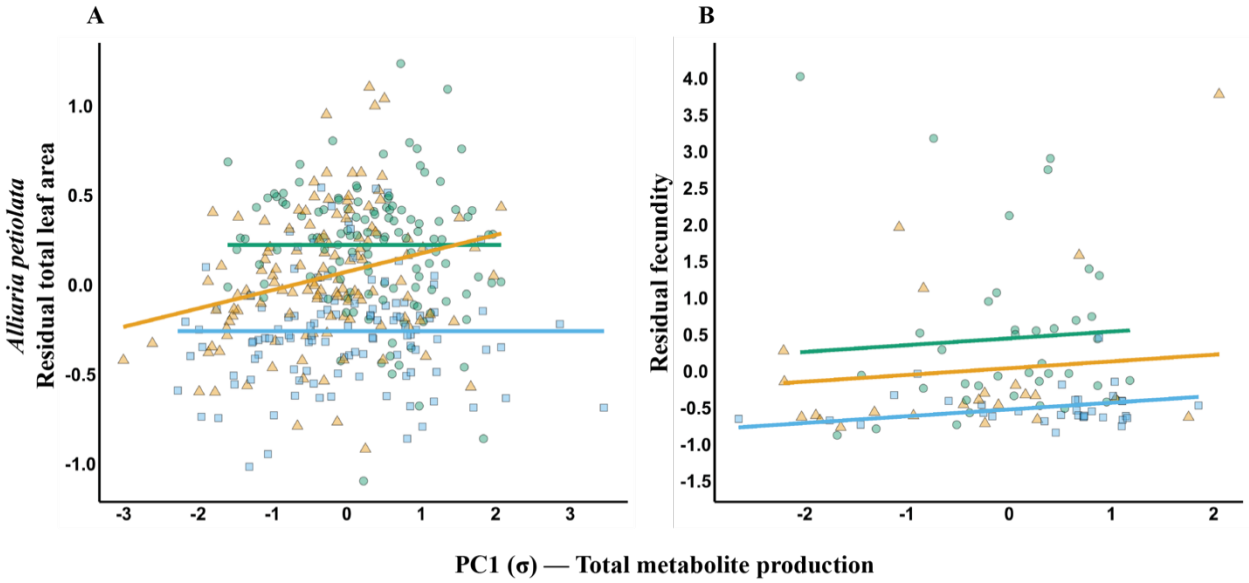

Figure 4. Selection gradients of PC1 (total metabolite production, denoting the production of Chl *a* and glucosinolates) for *A. petiolata* total leaf area (A) and fecundity (B). Green circles denote the alone treatment, orange triangles denote the interspecific treatment and blue squares denote the intraspecific treatment. The y-axis in panel A shows mean-standardized total leaf area (unitless), after controlling for *X. campestris* infection, fern abundance, greenhouse bench and *A. petiolata* transplant size. The y-axis in panel B shows mean-standardized fecundity after controlling for *A. petiolata* transplant size. Both x-axes show z-standardized *A. petiolata* PC1, representing the production of both glucosinolates and Chl *a*. Slopes of zero reflect non-significant selection gradients. Selection gradients are colored according to treatment.

Allelopathy-mediated selection on *A. petiolata* traits (path analysis)

PC1 and PC2 were significantly associated with TLA_{AS} in year 1, but not *A. saccharum* shoot mass in year 2. Therefore, TLA_{AS} was included in all path analyses as the intermediate step linking PC1 and PC2 to *A. petiolata* fitness. Significant predictors (as described in the results above) of *A. petiolata* TLA_{AP}, survival, fecundity and lifetime fitness were included as covariates

677 in path analyses of *A. petiolata* TLA_{AP}, survival, fecundity and lifetime fitness, respectively.
678 Significant predictors of *A. saccharum* TLA_{AS} were included in all path analyses.
679
680 In the TLA_{AP} path analysis, TLA_{AS} was negatively associated with TLA_{AP} ($\beta = -0.11$, $p < 0.05$).
681 The indirect effects of PC1 ($\beta = +0.02$) and PC2 ($\beta = -0.01$), through TLA_{AS}, on TLA_{AP} were
682 both significant (both $p < 0.01$); however, the direct effects of PC1 and PC2 on TLA_{AP} were not
683 ($p = 0.08$ and 0.19, respectively; Figure B1). Likewise, in the survival path analysis, TLA_{AS} was
684 also negatively associated with *A. petiolata* survival ($\beta = -0.38$, $p < 0.05$) and the indirect effects
685 of PC1 ($\beta = +0.07$, $p < 0.05$) and PC2 ($\beta = -0.05$, $p < 0.01$), through TLA_{AS}, on survival were
686 significant (Figure 5). Like in the TLA_{AP} path analysis, the direct effect of both PC1 and PC2 on
687 survival were not significant ($p = 0.83$ and 0.30, respectively). Both path analyses suggest that
688 PC1 and PC2 had opposite effects on *A. petiolata* fitness and only impacted fitness through their
689 intermediate effects on *A. saccharum*.
690
691 In contrast, TLA_{AS} was not associated with fecundity ($p = 0.92$) and there were no significant
692 direct or indirect effects of PC1 or PC2 on fecundity (Figure B2). Similarly, TLA_{AS} was not a
693 significant predictor in the path analysis of lifetime fitness ($p = 0.28$), and there were no indirect
694 effects of PC1 or PC2 on *A. petiolata* lifetime fitness. There was a significant direct effect of
695 PC2 on lifetime fitness ($\beta = -0.50$, $p < 0.05$), but not of PC1 ($p = 0.08$; Figure 6).
696

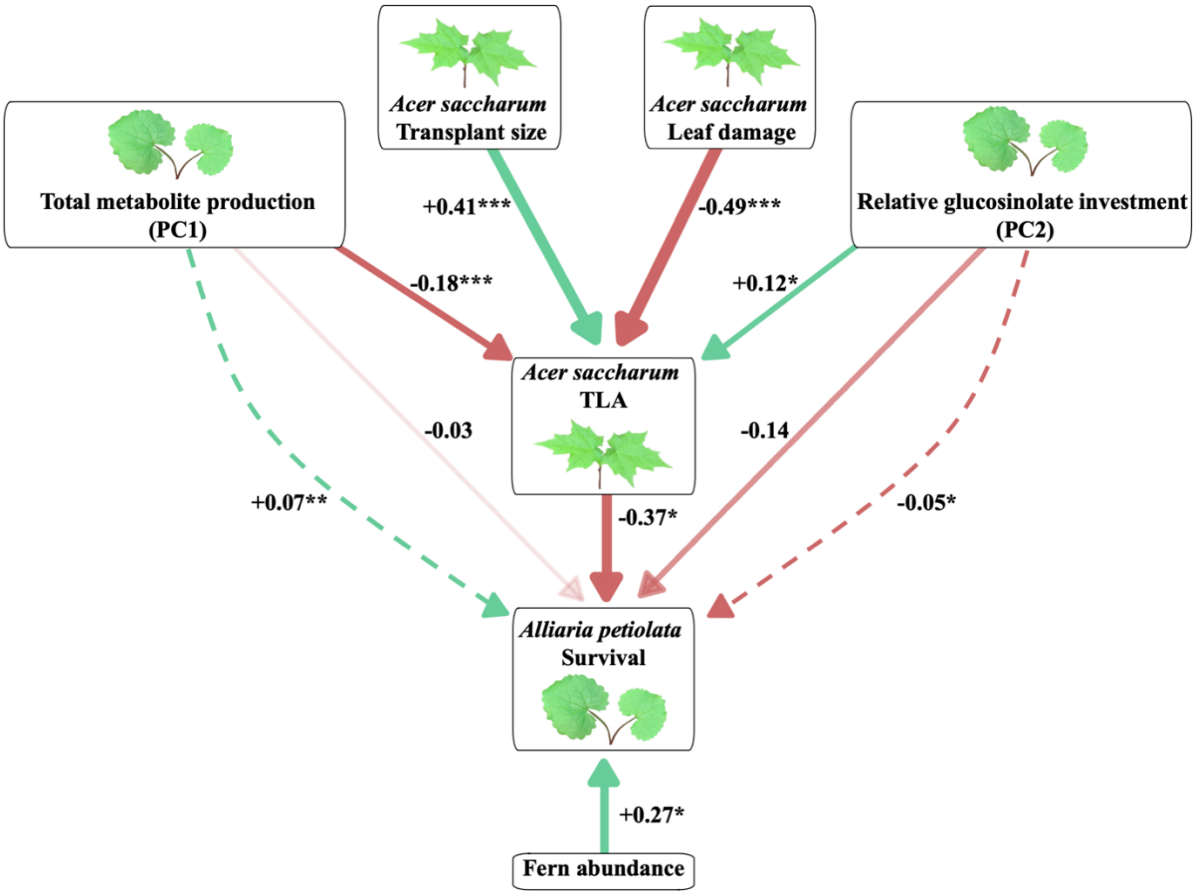

Figure 5. Path analysis of *Alliaria petiolata* survival. Survival was mean-standardized while other variables were z-standardized such that coefficients represent selection gradients. Arrows denote the direction of the effect, with green arrows indicating a positive gradient and red arrows indicate a negative gradient. Arrow thickness denotes the magnitude of the effect and darker arrows indicate greater significance. The text next to each arrow shows the path coefficient and its significance level ($p < 0.05$*, $p < 0.01$**, $p < 0.001$***). Total metabolite production (PC1) denotes the production of both glucosinolates and Chl *a*, while relative glucosinolate investment (PC2) indicates the production of glucosinolates relative to Chl *a*. *Acer saccharum* TLA denotes the total leaf area of *Acer saccharum* at the end of year 1. Solid arrows represent direct effects while dashed arrows represent indirect effects.

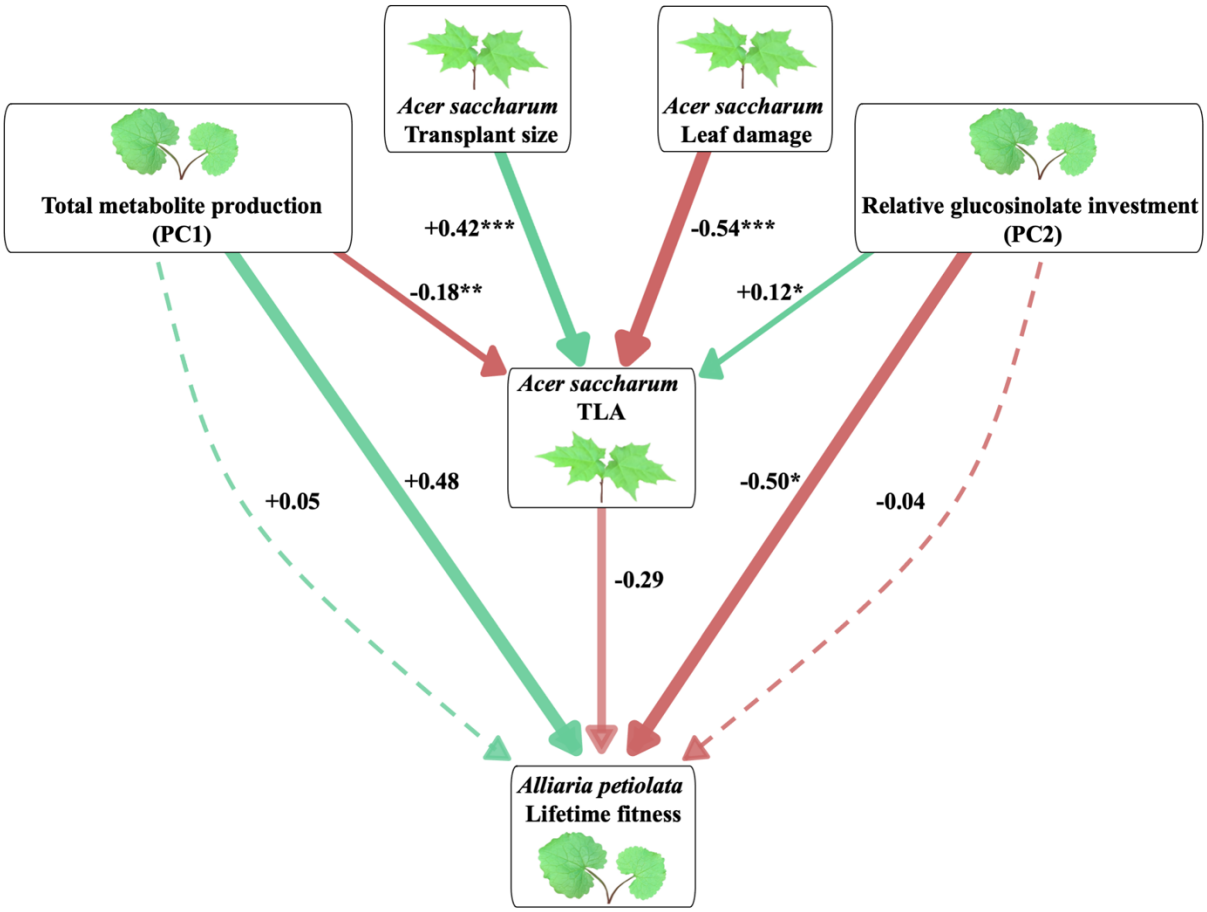

Figure 6. Path analysis of *Alliaria petiolata* lifetime fitness. Total fitness was mean-standardized while other variables were z-standardized to give SD-standardized selection gradients. Arrows denote the direction of the effect, with green arrows indicating a positive gradient and red arrows indicating a negative gradient. Arrow thickness denotes the magnitude of the effect and darker arrows indicate greater significance. The text next to each arrow shows the path coefficient and its significance level ($p < 0.05$*, $p < 0.01$**, $p < 0.001$***). Total metabolite production (PC1) denotes the production of both glucosinolates and Chl *a*, while relative glucosinolate investment (PC2) indicates the production of glucosinolates relative to Chl *a*. *Acer saccharum* TLA denotes the total leaf area of *Acer saccharum* at the end of year 1. Solid arrows represent direct effects while dashed arrows represent indirect effects.

721 **Discussion**

722 Plants that invade and spread across large geographical areas will experience heterogeneous
723 environments with variable ecological interactions including competition, herbivory, pathogen
724 damage, and abiotic stress (van Kleunen et al. 2018). In the Brassicaceae family, glucosinolates
725 play important roles in plant responses to biotic and abiotic stress (Holst and Fenwick 2003). To
726 investigate glucosinolate evolution and the potential for eco-evolutionary dynamics in
727 glucosinolate production via allelopathy, we quantified plasticity, heritability, and natural
728 selection via direct and indirect ecological effects across three competition treatments. We found
729 a strong, positive correlation between glucosinolate production and Chl *a* (Figure 2). Applying a
730 principal component analysis resulted in two statistically independent axes representing plastic
731 variation in total metabolite production (PC1), and heritable variation in relative glucosinolate
732 investment (PC2). PC1 was highly plastic across competition treatments with low levels of
733 among-family genetic variation, even though our experiment included a genotype from the
734 native range in Europe and populations spanning of ~3,000 km across Canada and the United
735 States, from Colorado and Georgia to Maine. In contrast, PC2 was highly heritable and did not
736 differ significantly among treatments (Table 2). Below we discuss the implications of this
737 heritable and plastic variation in glucosinolate production for the evolution of allelopathy during
738 *A. petiolata* invasion, and more generally for understanding the role of allelopathy in biological
739 invasion.
740
741 Several studies have examined allelopathic effects of glucosinolates in *A. petiolata* (Roberts and
742 Anderson 2001; Stinson et al. 2006; Burke 2008; Callaway et al. 2008; Wolfe et al. 2008; Barto
743 and Cipollini 2009; Barto et al. 2011; Cantor et al. 2011; Burke et al. 2019; Duchesneau et al.

744 2021; Roche et al. 2021). However, conclusions about the ecological impacts of allelopathy have
745 been mixed. For example, while several studies have found evidence that glucosinolates can
746 suppress competitors by inhibiting mycorrhizal colonization (Stinson et al. 2006; Callaway et al.
747 2008; Lankau et al. 2009; Evans et al. 2016), others have found no allelopathic effect (Burke
748 2008; Duchesneau et al. 2021). Population growth of *A. petiolata* depends on a variety of
749 ecological factors including germination time, fecundity, self-fertilization rates, and herbivory
750 (Davis et al. 2014; Kalisz et al. 2014; Burke et al. 2019). One hypothesis proposes that *A.*
751 *petiolata* evolves higher concentrations of allelopathic glucosinolates early in invasion, but lower
752 concentrations later in invasion as genotypes in growing populations experience stronger
753 intraspecific competition relative to interspecific competition (Lankau et al. 2009; Evans et al.
754 2016). In our opinion, these predictions are best tested by measuring selection gradients,
755 quantifying genetic constraints, and comparing direct versus indirect selection. However, no
756 previous study to our knowledge has applied the Chicago School of ecological genetics with
757 causal analysis to test these hypotheses in detail.
758
759 The eco-evolutionary feedbacks hypothesis makes three testable predictions that we evaluated
760 with our data. First, glucosinolate production should be highly heritable. Contrary to this
761 prediction, we found that glucosinolate production was highly plastic across competition
762 treatments, with relatively low heritability. Relative glucosinolate investment (PC2) was
763 significantly heritable, but only explained 16% of the variation in glucosinolates and Chl *a*.
764 Second, natural selection should favour genotypes with higher investment into glucosinolate
765 production when genotypes experience interspecific competition. Instead, we found that growth
766 of naïve *A. saccharum* saplings was promoted by genotypes with higher glucosinolate

767 investment (Figure 3), which had negative indirect effects on *A. petiolata* size and survival
768 (Figures 5, B1). In other words, natural selection under interspecific competition favors
769 genotypes that invest less into relative glucosinolate production, resulting in evolution for
770 reduced glucosinolate investment under interspecific competition. Third, natural selection should
771 favour genotypes with lower relative investment into glucosinolates when grown alone or under
772 intraspecific competition. Instead, we found that natural selection favors lower relative
773 investment in PC2 in all treatments, but perhaps less so when grown alone. Specifically, higher
774 PC2 was correlated with reduced survival in all treatments, and PC2 decreased by -0.22 σ and -
775 0.32 σ in the inter- and intra-specific treatments, respectively. Thus, none of our key results
776 support the hypothesis that competition dynamics during invasion create eco-evolutionary
777 feedbacks that maintain genetic variation in glucosinolate production.
778
779 Although we do not find evidence to support eco-evolutionary feedbacks mediated through
780 competition, the high level of phenotypic plasticity observed in PC1 is relevant to reconstructing
781 and predicting adaptive evolution during invasion of *A. petiolata*. Specifically, the univariate
782 response to natural selection (R) is a product of the narrow-sense heritability (h^2) and the strength
783 of natural selection (s). We calculated heritability in the broad sense (H^2), which as an upward-
784 biased estimate of narrow-sense heritability, and yet we found that H^2 for PC1 was non-
785 significant and low ($H^2 = 2.9$) relative to PC2 ($H^2 = 16.9$). Any biologically significant genetic
786 variation for PC1 was masked by high plasticity in our experiment, and ecological conditions in
787 natural populations are likely more variable than our relatively controlled greenhouse and field
788 gardens, which would further decrease heritability. We therefore conclude that the evolutionary
789 potential of PC1 is weak. Instead, *A. petiolata* glucosinolate and Chl *a* production is primarily

environment-dependent, representing a highly plastic strategy that may contribute to its rapid proliferation in North America.

The significant and high heritability we observed for PC2 is also relevant to reconstructing and predicting evolution in *A. petiolata*. PC2 was negatively correlated with survival in all treatments, consistent with an evolutionary cost to glucosinolate investment that is elevated under interspecific competition. The cost that we observe would favor populations with lower investment into glucosinolates. It is therefore unlikely that genetic variation across our experimental populations has been maintained by selection for allelopathy. Instead, the maintenance of genetic variation despite fitness costs suggests that glucosinolates play other important ecological roles. For example, the evolution of increased competitive ability (EICA) hypothesis predicts an evolutionary reallocation of resources from defense to growth and competition in introduced populations that escape their natural enemies (Blossey and Notzold 1995). Indeed, *A petiolata* has relatively few natural enemies in North America compared to Europe (Rodgers et al. 2008), and total glucosinolate production in North America was estimated to be 36% lower than native European populations (Cipollini et al. 2005). This hypothesis does not explain the significant level of heritability observed in relative glucosinolate investment (PC2) across populations. Instead, it is possible that herbivory is heterogenous over space and time within the introduced range, maintaining genetic variation in glucosinolate investment. Glucosinolates also play a variety of other ecological roles including stress adaptation (Louda and Mole 1991). Testing these hypotheses is beyond the scope of our experiment, but the same seed families that we used are available from the Global Garlic Mustard Field Survey (Colautti et al. 2014) to enable future studies.

813

814 Our study focused on total shoot glucosinolates as a high-throughput and non-destructive
815 measure of glucosinolate production, allowing us to also measure lifetime fitness for the same
816 individuals. While allelopathy may be mediated through root exudates, our approach is
817 consistent with previous studies demonstrating allelopathy in *A. petiolata* using either leaf or
818 whole plant extracts as glucosinolate concentrations are likely correlated among tissues of the
819 same plant (McCarthy and Hanson 1998; Roberts and Anderson 2001; Stinson et al. 2006;
820 Callaway et al. 2008). While sinigrin is secreted through roots and suspected to be the causal
821 agent of allelopathy in *A. petiolata* (Cantor et al. 2011; Evans et al. 2016), it is also the most
822 abundant glucosinolate in *A. petiolata* (Vaughn and Berhow 1999; Haribal and Renwick 2001)
823 and therefore should be correlated with our estimates of total glucosinolates.

824

825 In summary, we examined plasticity, heritability, and natural selection of glucosinolate
826 production in one native and 22 introduced populations of *A. petiolata*, reared in three
827 competition treatments in greenhouse and field common gardens. We found that most traits were
828 highly plastic, and selection consistently favored genotypes that invest less into glucosinolate
829 production relative to Chl *a* under interspecific competition. We conclude that eco-evolutionary
830 feedbacks involving competition have not likely played a significant role in the invasion of *A.*
831 *petiolata* across eastern North America. Instead, the successful spread of this species more likely
832 owes to preadapted traits and phenotypic plasticity. Although not involved in competition,
833 glucosinolates likely play other ecological roles during invasion that can be tested with seed
834 accessions available from the Global Garlic Mustard Field Survey. More generally, our results

demonstrate how evolution during biological invasion can be better understood through the application of quantitative genetics and causal analysis.

Author Contributions

RH and RIC conceived and designed the experiment. RH and MM ran the experiment with financial support and assistants provided by RIC. RH led the data analysis manuscript writing with contributions from MM, and writing guidance from RIC.

Acknowledgements

The authors are grateful to Mabel Fuentes, Damien Felstead, Logan Wisteard, Jacob Stollman, Claire Smith, and Evelyn Newman for helping with experiment set up, sample processing and data collection. We are also grateful to Dr. Bonier and Dr. Aarssen for their time, feedback, and insights in reviewing the manuscript. Funding was provided to RIC from NSERC Discovery and from a CFI Tier II Canada Research Chair.

Data Availability

Our data are available through Dryad (LINK).

References

Alabi N, Wu Y, Bossdorf O, Rieseberg LH, Colautti RI. 2021. Genome report: A draft genome of Alliaria petiolata (garlic mustard) as a model system for invasion genetics. G3 Genes, Genomes, Genet. 11(12). doi:10.1093/g3journal/jkab339.

Anderson H. 2012. Invasive garlic mustard (Alliaria petiolata) best management practices in Ontario. Peterborough, Ontario.

Anderson RC, Dhillion SS, Kelley TM. 1996. Aspects of the ecology of an invasive plant, garlic mustard (Alliaria petiolata), in Central Illinois. Restor Ecol. 4(2):181–191.

861 doi:10.1111/j.1526-100X.1996.tb00118.x.

862 Baker HG, Stebbins GL. 1965. The genetics of colonizing species: Proceedings of the first
863 International Union of Biological Sciences symposium on general biology. Baker HG,
864 Stebbins GL, editors. New York: Academic Press.

865 Barrett SCH. 2016. Foundations of invasion genetics: the Baker and Stebbins legacy. In: Barrett
866 SCH, Colautti RI, Dlugosch KM, Rieseberg LH, editors. Invasion Genetics: The Baker and
867 Stebbins Legacy. Wiley-Blackwell. p. 1–19.

868 Barto K, Antunes P, Stinson K, Koch AM, Klironomos JN, Cipollini D. 2011. Differences in
869 arbuscular mycorrhizal fungal communities associated with sugar maple seedlings in and
870 outside of invaded garlic mustard forest patches. Biol Invasions. 13(12):2755–2762.
871 doi:10.1007/s10530-011-9945-6.

872 Barto K, Cipollini D. 2009. Half-lives and field soil concentrations of Alliaria petiolata
873 secondary metabolites. Chemosphere. 76(1):71–75.
874 doi:10.1016/j.chemosphere.2009.02.020.

875 Berry JC, Fahlgren N, Pokorny AA, Bart RS, Veley KM. 2018. An automated, high-throughput
876 method for standardizing image color profiles to improve image-based plant phenotyping.
877 PeerJ. doi:10.7717/peerj.5727.

878 Blossey B, Notzold R. 1995. Evolution of increased competitive ability in invasive
879 nonindigenous plants: A hypothesis. J Ecol. 83(5):887–889. doi:10.2307/2261425.

880 Bradski G. 2000. The OpenCV Library. Dr Dobb's J Softw Tools. 120:122–125.

881 Brooks ME, Kristensen K, van Benthem KJ, Magnusson A, Berg CW, Nielsen A, Skaug HJ,
882 Mächler M, Bolker BM. 2017. glmmTMB balances speed and flexibility among packages
883 for zero-inflated generalized linear mixed modeling. R J. 9:378–400. doi:10.32614/rj-2017-

884 066.

885 Burke DJ. 2008. Effects of Alliaria petiolata (garlic mustard; Brassicaceae) on mycorrhizal
886 colonization and community structure in three herbaceous plants in a mixed deciduous
887 forest. Am J Bot. 95(11):1416–1425. doi:10.3732/ajb.0800184.

888 Burke DJ, Carrino-Kyker SR, Hoke A, Cassidy S, Bialic-Murphy L, Kalisz S. 2019. Deer and
889 invasive plant removal alters mycorrhizal fungal communities and soil chemistry: Evidence
890 from a long-term field experiment. Soil Biol Biochem. 128:13–21.
891 doi:10.1016/j.soilbio.2018.09.031. https://doi.org/10.1016/j.soilbio.2018.09.031

892 Callaway RM, Cipollini D, Barto K, Thelen GC, Hallett SG, Prati D, Stinson K, Klironomos J.
893 2008. Novel weapons: Invasive plant suppresses fungal mutualists in America but not in its
894 native Europe. Ecology. 89(4):1043–1055. doi:10.1890/07-0370.1.

895 Callaway RM, Ridenour WM. 2004. Novel weapons: Invasive success and the evolution of
896 increased competitive ability. Front Ecol Environ. 2(8):436–443. doi:10.1890/1540-
897 9295(2004)002[0436:NWISAT]2.0.CO;2.

898 Cantor A, Hale A, Aaron J, Traw MB, Kalisz S. 2011. Low allelochemical concentrations
899 detected in garlic mustard-invaded forest soils inhibit fungal growth and AMF spore
900 germination. Biol Invasions. 13:3015–3025. doi:10.1007/s10530-011-9986-x.

901 Cavers PB, Heagy MI, Kokron RF. 1979. The Biology of Canadian Weeds.: 35. Alliaria petiolata
902 (M. Bieb.) Cavara and Grande. Can J Plant Sci. 59:217–229. doi:10.4141/cjps79-029.

903 Chen YZ, Pang QY, He Y, Zhu N, Branstrom I, Yan XF, Chen S. 2012. Proteomics and
904 metabolomics of arabidopsis responses to perturbation of glucosinolate biosynthesis. Mol
905 Plant. 5:1138–1150. doi:10.1093/mp/sss034.

906 Ciola V, Cipollini D. 2011. Distribution and host range of a powdery mildew fungus infecting

907 garlic mustard, alliaria petiolata, in Southwestern Ohio. Am Midl Nat. 166:40–52.
908 doi:10.1674/0003-0031-166.1.40.
909 Cipollini D. 2002. Variation in the expression of chemical defenses in Alliaria Petiolata
910 (Brassicaceae) in the field and common garden. Am J Bot. 89(9):1422–1430.
911 doi:10.3732/ajb.89.9.1422.
912 Cipollini D, Gruner B. 2007. Cyanide in the chemical arsenal of garlic mustard, Alliaria
913 petiolata. J Chem Ecol. 33(1):85–94. doi:10.1007/s10886-006-9205-x.
914 Cipollini D, Mbagwu J, Barto K, Hillstrom C, Enright S. 2005. Expression of constitutive and
915 inducible chemical defenses in native and invasive populations of Alliaria petiolata. J Chem
916 Ecol. 31:1255–1267. doi:10.1109/tmtt.2013.2247619.
917 Colautti R, Franks SJ, Hufbauer RA, Hufbauer RA, Kotanen PM, Torchin M, Byers JE, Pyšek P,
918 Bossdorf O. 2014. The global garlic mustard field survey (GGMFS): challenges and
919 opportunities of a unique, large-scale collaboration for invasion biology. NeoBiota. 21:29–
920 47. doi:10.3897/neobiota.21.5242.
921 Colautti RI, Barrett SCH. 2011. Population divergence along lines of genetic variance and
922 covariance in the invasive plant Lythrum salicaria in eastern North America. Evolution (N
923 Y). 65(9):2514–2529. doi:10.1111/j.1558-5646.2011.01313.x.
924 Colautti RI, Barrett SCH. 2013. Rapid adaptation to climate facilitates range expansion of an
925 invasive plant. Science (80-). 342(6156):364–366. doi:10.1126/science.1242121.
926 Colautti RI, Lau JA. 2015. Contemporary evolution during invasion: Evidence for
927 differentiation, natural selection, and local adaptation. Mol Ecol. 24(9):1999–2017.
928 doi:10.1111/mec.13162.
929 Colautti RI, Maron JL, Barrett SCH. 2009. Common garden comparisons of native and

introduced plant populations: Latitudinal clines can obscure evolutionary inferences. Evol Appl. 2(2):187–199. doi:10.1111/j.1752-4571.2008.00053.x.

Conner JK, Hartl DL. 2004. A primer of ecological genetics. Oxford University Press.

Crawley MJ. 2007. The R Book. 2nd ed. Chichester, West Sussex, United Kingdom: Wiley.

Cruden RW, McClain AM, Shrivastava GP. 1996. Pollination biology and breeding system of Alliaria petiolata (Brassicaceae). Bull Torrey Bot Club. 123:273–280. doi:10.2307/2996775.

Davis MA, MacMillen C, LeFevre-Levy M, Dallavalle C, Kriegel N, Tyndel S, Martinez Y, Anderson MD, Dosch JJ. 2014. Population and plant community dynamics involving garlic mustard (Alliaria petiolata) in a Minnesota Oak Woodland: a four year study. J Torrey Bot Soc. 141(3):205–216. doi:10.3159/torrey-d-13-00062.1.

Dlugosch KM, Parker IM. 2008. Founding events in species invasions: Genetic variation, adaptive evolution, and the role of multiple introductions. Mol Ecol. 17(1):431–449. doi:10.1111/j.1365-294X.2007.03538.x.

Doorduin LJ, Vrieling K. 2011. A review of the phytochemical support for the shifting defence hypothesis. Phytochem Rev. 10(1):99–106. doi:10.1007/s11101-010-9195-8.

Duchesneau K, Golemiec A, Colautti RI, Antunes PM. 2021. Functional shifts of soil microbial communities associated with Alliaria petiolata invasion. Pedobiologia (Jena). 84(August 2020):150700. doi:10.1016/j.pedobi.2020.150700. https://doi.org/10.1016/j.pedobi.2020.150700

Durka W, Bossdorf O, Prati D, Auge H. 2005. Molecular evidence for multiple introductions of garlic mustard (Alliaria petiolata, Brassicaceae) to North America. Mol Ecol. 14(6):1697–1706. doi:10.1111/j.1365-294X.2005.02521.x.

953 Endler J. 1986. Natural selection in the wild, Volume 21. Princeton University Press.

954 Evans JA, Lankau RA, Davis AS, Raghu S, Landis DA. 2016. Soil-mediated eco-evolutionary
955 feedbacks in the invasive plant Alliaria petiolata. Funct Ecol. 30(7):1053–1061.
956 doi:10.1111/1365-2435.12685.

957 Godman R, Yawney H, Tubbs C. 1990. Acer saccharum Marsh. Sugar maple. In: Burns RM,
958 Honkala BH, editors. Silvics of North America: Hardwoods. Washington: Timber
959 Management Research. p. 78–87.

960 Gomes MP, Garcia QS, Barreto LC, Lucia PPS, Matheus MT, Figueredo CC. 2017. Allelopathy:
961 an overview from micro- to macroscopic organisms, from cells to environments, and the
962 perspectives in a climate-changing world. Biologia (Bratisl). 72(2):113–129.

963 Hajduk GK, Walling CA, Cockburn A, Kruuk LEB. 2020. The algebra of evolution : The
964 robertson-price identity and viability selection for body mass in a wild bird population.
965 Philos Trans R Soc B Biol Sci. 375:20190359. doi:10.1098/rstb.2019.0359.

966 Haribal M, Renwick JAA. 2001. Seasonal and population variation in flavonoid and alliarinoside
967 content of Alliaria petiolata. J Chem Ecol. 27(8):1585–1594.
968 doi:10.1023/A:1010406224265.

969 Hierro JL, Callaway RM. 2021. The Ecological Importance of Allelopathy. Annu Rev Ecol Evol
970 Syst. 52:25–45. doi:10.1146/annurev-ecolsys-051120-030619.

971 Holst B, Fenwick GR. 2003. Glucosinolates. In: Caballero B, editor. Encyclopedia of Food
972 Sciences and Nutrition. 2nd ed. Academic Press. p. 2922–2930.

973 Hopkins W, Hüner N. 2009. Secondary metabolites. In: Introduction to plant physiology. 4th ed.
974 Wiley.

975 Inderjit, Seastedt TR, Callaway RM, Pollock JL, Kaur J. 2008. Allelopathy and plant invasions:

Traditional, congeneric, and bio-geographical approaches. Biol Invasions. 10:875–890. doi:10.1007/s10530-008-9239-9.

Inderjit, Simberloff D, Kaur H, Kalisz S, Bezemer TM. 2021. Novel chemicals engender myriad invasion mechanisms. New Phytol. 232(3):1184–1200. doi:10.1111/nph.17685.

Ishida M, Kakizaki T, Ohara T, Morimitsu Y. 2011. Development of a simple and rapid extraction method of glucosinolates from radish roots. Breed Sci. 61(2):208–211. doi:10.1270/jsbbs.61.208.

Ishida M, Nagata M, Ohara T, Kakizaki T, Hatakeyama K, Nishio T. 2012. Small variation of glucosinolate composition in Japanese cultivars of radish (Raphanus sativus L.) requires simple quantitative analysis for breeding of glucosinolate component. Breed Sci. 62(1):63–70. doi:10.1270/jsbbs.62.63.

Kalisz S, Spigler RB, Horvitz CC. 2014. In a long-term experimental demography study, excluding ungulates reversed invader's explosive population growth rate and restored natives. Proc Natl Acad Sci. 111(12):4501–4506. doi:10.1073/pnas.1310121111.

Keane RM, Crawley MJ. 2002. Exotic plant invasions and the enemy release hypothesis. Trends Ecol Evol. 17(4):164–170. doi:10.1016/S0169-5347(02)02499-0.

Kingsolver JG, Schemske DW. 1991. Path analyses of selection. Trends Ecol Evol. 6(9):276–280. doi:10.1016/0169-5347(91)90004-H.

van Kleunen M, Bossdorf O, Dawson W. 2018. The ecology and evolution of alien plants. Annu Rev Ecol Evol Syst. 49:25–47. doi:10.1146/annurev-ecolsys-110617-062654.

Kueffer C, Pyšek P, Richardson DM. 2013. Integrative invasion science: Model systems, multi-site studies, focused meta-analysis and invasion syndromes. New Phytol. 200(3):615–633. doi:10.1111/nph.12415.

999 Lande R, Arnold SJ. 1983. The measurement of selection on correlated characters. Evolution (N
1000 Y). 37:1210–1226. doi:10.2307/2408842.
1001 Lankau RA, Nuzzo V, Spyreas G, Davis AS. 2009. Evolutionary limits ameliorate the negative
1002 impact of an invasive plant. Proc Natl Acad Sci. 106(36):15362–15367.
1003 doi:10.1073/pnas.0905446106.
1004 Louda S, Mole S. 1991. Glucosinolates: Chemistry and ecology. In: Rosenthal GA, Berenbaum
1005 MR, editors. Herbivores: Their interactions with secondary plant metabolites, Volume 1:
1006 The chemical participants. 2nd ed. Academic Press. p. 123–157.
1007 Lynch M, Walsh B. 1998. Genetics and Analysis of Quantitative Traits. Sinauer.
1008 Matsumura S, Arlinghaus R, Dieckmann U. 2012. Standardizing selection strengths to study
1009 selection in the wild: A critical comparison and suggestions for the future. Bioscience.
1010 62:1039–1054. doi:10.1525/bio.2012.62.12.6.
1011 Mawlong I, Sujith Kumar MS, Gurung B, Singh KH, Singh D. 2017. A simple
1012 spectrophotometric method for estimating total glucosinolates in mustard de-oiled cake. Int
1013 J Food Prop. 20(12):3274–3281. doi:10.1080/10942912.2017.1286353.
1014 McCarthy BC, Hanson SL. 1998. An assessment of the allelopathic potential of the invasive
1015 weed Alliaria petiolata (Brassicaceae). Castanea. 63:68–73.
1016 Misyura M, Colasanti J, Rothstein SJ. 2013. Physiological and genetic analysis of Arabidopsis
1017 thaliana anthocyanin biosynthesis mutants under chronic adverse environmental conditions.
1018 J Exp Bot. 64:229–240. doi:10.1093/jxb/ers328.
1019 Mullarkey AA, Byers DL, Anderson RC. 2013. Inbreeding depression and partitioning of genetic
1020 load in the invasive biennial Alliaria petiolata (Brassicaceae). Am J Bot. 100(3):509–518.
1021 doi:10.3732/ajb.1200403.

1022 Müller-Schärer H, Schaffner U, Steinger T. 2004. Evolution in invasive plants: Implications for
1023 biological control. Trends Ecol Evol. 19(8):417–422. doi:10.1016/j.tree.2004.05.010.
1024 Ochocki BM, Miller TEX. 2017. Rapid evolution of dispersal ability makes biological invasions
1025 faster and more variable. Nat Commun. 8. doi:10.1038/ncomms14315.
1026 Parker IM, Rodriguez J, Loik ME. 2003. An evolutionary approach to understanding the biology
1027 of invasions: Local adaptation and general-purpose genotypes in the weed Verbascum
1028 thapsus. Conserv Biol. 17(1):59–72. doi:10.1046/j.1523-1739.2003.02019.x.
1029 Philips BL, Brown GP, Webb JK, Shine R. 2006. Invasion and the evolution of speed in toads.
1030 Nat Commun. 439:1–2.
1031 Python Core Team. 2015. Python: A dynamic, open source programming language. Python
1032 Softw Found. doi:10.1109/8.121596.
1033 Qian L, Qian W, Snowdon RJ. 2016. Haplotype hitchhiking promotes trait coselection in
1034 Brassica napus. Plant Biotechnol J. 14:1578–1588. doi:10.1111/pbi.12521.
1035 R Core Team. 2020. R: A language and environment for statistical computing. Vienna, Austria.
1036 https://www.r-project.org/
1037 Ralph N. 1998. Sugar maple: Its characteristics and potentials. In: Horsley S, Long R, editors.
1038 Sugar maple ecology and health, proceedings of an international symposium. Pennsylvania:
1039 USDA Forest Service, Northeastern Research Station. p. 1–14.
1040 Richards CL, Bossdorf O, Muth NZ, Gurevitch J, Pigliucci M. 2006. Jack of all trades, master of
1041 some? On the role of phenotypic plasticity in plant invasions. Ecol Lett. 9(8):981–993.
1042 doi:10.1111/j.1461-0248.2006.00950.x.
1043 Ritchie RJ. 2006. Consistent sets of spectrophotometric chlorophyll equations for acetone,
1044 methanol and ethanol solvents. Photosynth Res. 89:27–41. doi:10.1007/s11120-006-9065-9.

1045 Roberts KJ, Anderson RC. 2001. Effect of garlic mustard [Alliaria petiolata (Beib. Cavara &
1046 Grande)] extracts on plants and arbuscular mycorrhizal (AM) fungi. Am Midl Nat.
1047 146:146–152. doi:10.1674/0003-0031(2001)146[0146:EOGMAP]2.0.CO;2.
1048 Roche MD, Pearse IS, Bialic-Murphy L, Kivlin SN, Sofaer HR, Kalisz S. 2021. Negative effects
1049 of an allelopathic invader on AM fungal plant species drive community-level responses.
1050 Ecology. 102(1):e03201. doi:10.1002/ecy.3201.
1051 Rodgers VL, Scanga SE, Kolozsvary MB, Garneau DE, Kilgore JS, Anderson LJ, Hopfensperger
1052 KN, Aguilera AG, Urban RA, Juneau KJ. 2022. Where is Garlic Mustard? Understanding
1053 the ecological context for invasions of Alliaria petiolata. Bioscience. 72(6):521–537.
1054 doi:10.1093/biosci/biac012.
1055 Rodgers VL, Stinson KA, Finzi AC. 2008. Ready or not, Garlic Mustard is moving in: Alliaria
1056 petiolata as a member of Eastern North American forests. Bioscience. 58(5):426–436.
1057 doi:10.1641/b580510.
1058 Rosseel Y. 2012. lavaan: An R Package for Structural Equation Modeling. J Stat Softw. 48(2):1–
1059 36.
1060 Sax D, Brown JH. 2011. The paradox of invasion. Glob Ecol Biogeogr. 9(5):363–371.
1061 Scheiner SM, Mitchell RJ, Callahan HS. 2000. Using path analysis to measure natural selection.
1062 J Evol Biol. 13(3):423–433. doi:10.1046/j.1420-9101.2000.00191.x.
1063 Shine R, Alford RA, Blennerhasset R, Brown GP, DeVore JL, Ducatez S, Finnerty P, Greenlees
1064 M, Kaiser SW, McCann S, et al. 2021. Increased rates of dispersal of free-ranging cane
1065 toads (Rhinella marina) during their global invasion. Sci Rep. 11(1):1–9.
1066 doi:10.1038/s41598-021-02828-5. https://doi.org/10.1038/s41598-021-02828-5
1067 Shipley B. 2016. Cause and correlation in biology. 2nd ed. Shipley B, editor. Cambridge

University Press.

Smith LM. 2015. Garlic mustard (Alliaria petiolata) glucosinolate content varies across a natural light gradient. J Chem Ecol. 41:486–492. doi:10.1007/s10886-015-0580-z.

Sosnoskie LM, Cardina J. 2009. Laboratory methods for breaking dormancy in Garlic Mustard (Alliaria petiolata) seeds. Invasive Plant Sci Manag. 2(2):185–189. doi:10.1614/ipsm-08-126.1.

Stinson KA, Campbell SA, Powell JR, Wolfe BE, Callaway RM, Thelen GC, Hallett SG, Prati D, Klironomos JN. 2006. Invasive plant suppresses the growth of native tree seedlings by disrupting belowground mutualisms. PLoS Biol. 12(2). doi:10.1371/journal.pbio.0040140.

Szücs M, Vahsen ML, Melbourne BA, Hoover C, Weiss-Lehman C, Hufbauer RA, Schoener TW. 2017. Rapid adaptive evolution in novel environments acts as an architect of population range expansion. Proc Natl Acad Sci U S A. 114(51):13501–13506. doi:10.1073/pnas.1712934114.

Uesugi A, Kessler A. 2013. Herbivore exclusion drives the evolution of plant competitiveness via increased allelopathy. New Phytol. 198(3):916–924. doi:10.1111/nph.12172.

Vaughn SF, Berhow MA. 1999. Allelochemicals isolated from tissues of the invasive weed garlic mustard (Alliaria petiolata). J Chem Ecol. 25:2495–2504. doi:10.1023/A:1020874124645.

Vicente JG, Holub EB. 2013. Xanthomonas campestris pv. Campestris (cause of black rot of crucifers) in the genomic era is still a worldwide threat to brassica crops. Mol Plant Pathol. 14(1):2–18. doi:10.1111/j.1364-3703.2012.00833.x.

Williams JL, Kendall BE, Levine JM. 2016. Rapid evolution accelerates plant population spread in fragmented experimental landscapes.pdf. Science (80-). 353.

1091 doi:10.1126/science.aaf6268.

1092 Wolfe BE, Rodgers VL, Stinson KA, Pringle A. 2008. The invasive plant Alliaria petiolata

1093 (garlic mustard) inhibits ectomycorrhizal fungi in its introduced range. J Ecol. 96:777–783.

1094 doi:10.1111/j.1365-2745.2008.0.

1095 Wu YI, Lougheed D, Lougheed SC, Moniz K, Walker VK, Colautti RI. 2020. baRcodeR: An

1096 open-source R package for sample labelling. Methods Ecol Evol. 11:980–985.

1097 doi:10.1111/2041-210X.13405.

1098

Supporting Information for Honor, Marcellus and Colautti "Direct and indirect fitness effects of competition limit evolution of allelopathy in an invading plant"

27-June-2023

Appendix A (Methods)

Machine learning analysis of plant size

To measure rosette size in *Alliaria petiolata*, we trained a machine learning model of whole plant images. The top and side of each *A. petiolata* rosette were photographed using two webcams affixed to a custom image-capture stand (Figure A4). Cameras were oriented to image the top and side of each rosette to capture leaf area in all three dimensions. We measured relative plant size as the total pixel area of each plant, given that cameras were fixed at a constant distance from each imaged plant, (Figure A5).

Image analysis was performed using a custom machine learning algorithm written in Python 3.8 using the packages OpenCV2 and PlantCV2 (Bradski 2000; Python Core Team 2015; Berry et al. 2018). We first trained the computer to identify leaves based on the color spectrum of each pixel captured by the camera, encoded on an rgb scale (0-255). In a subset of 100 training images, we manually assigned 10 pixels in each image as leaves or background. From this training set, a Naïve Bayesian classifier algorithm available in the PlantCV2 package could assign a posterior probability of leaf vs background to all pixels in the remaining images.

A subset of 76 plants were used to verify the ML estimates. For these plants, total leaf area (TLA) was estimated manually by estimating the area of each leaf (length times width) and summing across all leaves for each plant. There was a strong correlation between rosette size (measured as the total number of pixels in an image corresponding to plant) and TLA ($p < 0.001$, $R^2=0.852$), which allowed us to automate measurements of all 5,659 photos. Each photo that was analyzed produced an output image, outlining the parts identified as rosette (i.e., Figure A5). Each of the 5,659 images were manually inspected to check for assignment errors in the machine learning algorithm. We found that 29 plants were mis-identified. In these instances, we sampled pixels directly from the mis-identified images and retrained the machine learning algorithm on these pixels until all plants were correctly identified.

We wrote a program in Python 3.8 to automate image capture. This program displays webcam images to assist with correct placement of each plant, allows the user to take a photo with each camera, and displays the photos for manual quality inspection. If approved by the user, the images are automatically stored and named with the appropriate identification (as read through a barcode scanner) and the exact time that the photos were taken. We used Unix time, which is the number of seconds since Jan 1st, 1970, providing a precise time of measurement with which we could calculate growth rates with high accuracy.

Secondary compound processing and analysis

Two frozen leaf punches (8mm diameter) were pulverized in 1.5mL centrifuge tubes using a Next Advance Bullet Blender®. Two cycles of 15s on the highest power (12) were performed

46 and samples were submerged in liquid N_2 before and after each cycle. Samples were kept frozen
47 to inhibit enzymatic degradation of target compounds. Leaf tissue was then extracted in 0.55mL
48 of 100% methanol, incubated for 1 hour at 25°C and 300rpm, and subsequently centrifuged for 2
49 minutes at 2500g (Eppendorf, 5427 R). Next, the pellet was discarded and 485µL of supernatant
50 was stored at –80°C until further processing. The concentration of total glucosinolates and Chl *a*
51 were determined using 96 well assays with spectrophotometric analysis. Two technical replicates
52 were measured for each composite sample of leaf tissue.
53
54 Chl *a* was measured by transferring 20µL of sample extract into the wells of a 96 well UV flat
55 bottom plate; the sample was then evaporated and resuspended in 50µL of 100% methanol
56 immediately prior to reading. Total glucosinolate concentration was evaluated by rinsing 465µL
57 of extract with 650µL of hexane to remove other pigments or secondary compounds that may
58 interfere with analysis. To rinse, samples were placed on an incubator at 30°C for 25 minutes at
59 600rpm. Samples were then chilled in an ice bath for 15 minutes and subsequently centrifuged at
60 2500g for 10 minutes at 4°C. We then transferred 100µL of the sample into the wells of a 96
61 well UV flat bottom plate, left samples to evaporate and resuspended them in 100µL of 100%
62 methanol immediately prior to reading. The assays were read at 425nm before and after adding
63 100µL of 3.5 mM sodium tetrachloropalladate ($NaCl_4Pd$) to wells.
64
65
66

Figure A1. *Alliaria petiolata* grown in the (A) alone treatment (B) intraspecific competition treatment and (c) interspecific competition treatment.

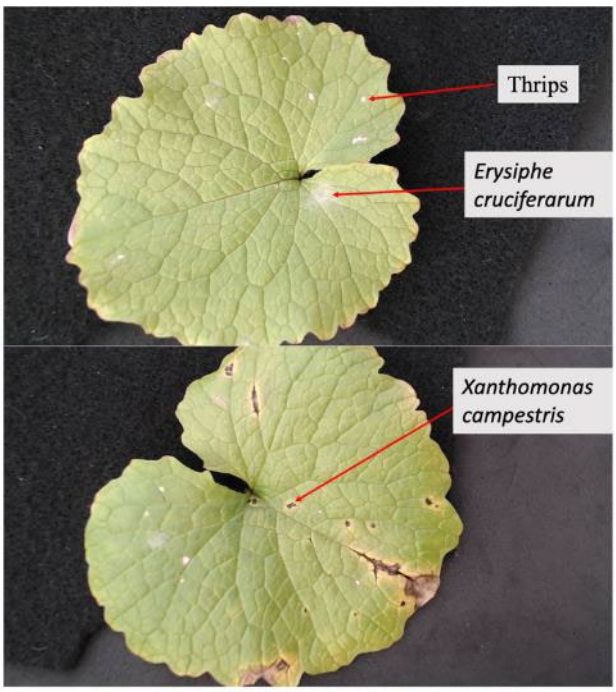

Figure A2. Examples of leaf images used to measure pathogen data.

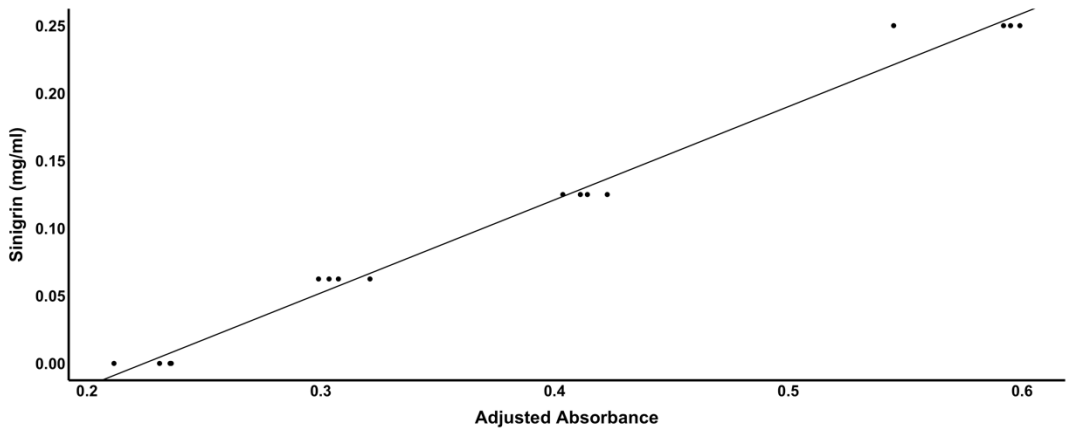

Figure A3. Standard curve of sinigrin concentration. $\mathbf{Sinigrin\ (mg/ml)} = \mathbf{0.69}\left(\boldsymbol{A_2} - \frac{\boldsymbol{A_1}}{\mathbf{2}}\right) - \mathbf{0.15}$, Where $\boldsymbol{A}$ is the absorbance at 425 nm and subscripts denote before ($\boldsymbol{A_1}$) and after $NaCl_4Pd$ was added ($\boldsymbol{A_2}$).

Figure A4. Example of greenhouse and photo apparatus used to capture images for growth rate analysis.

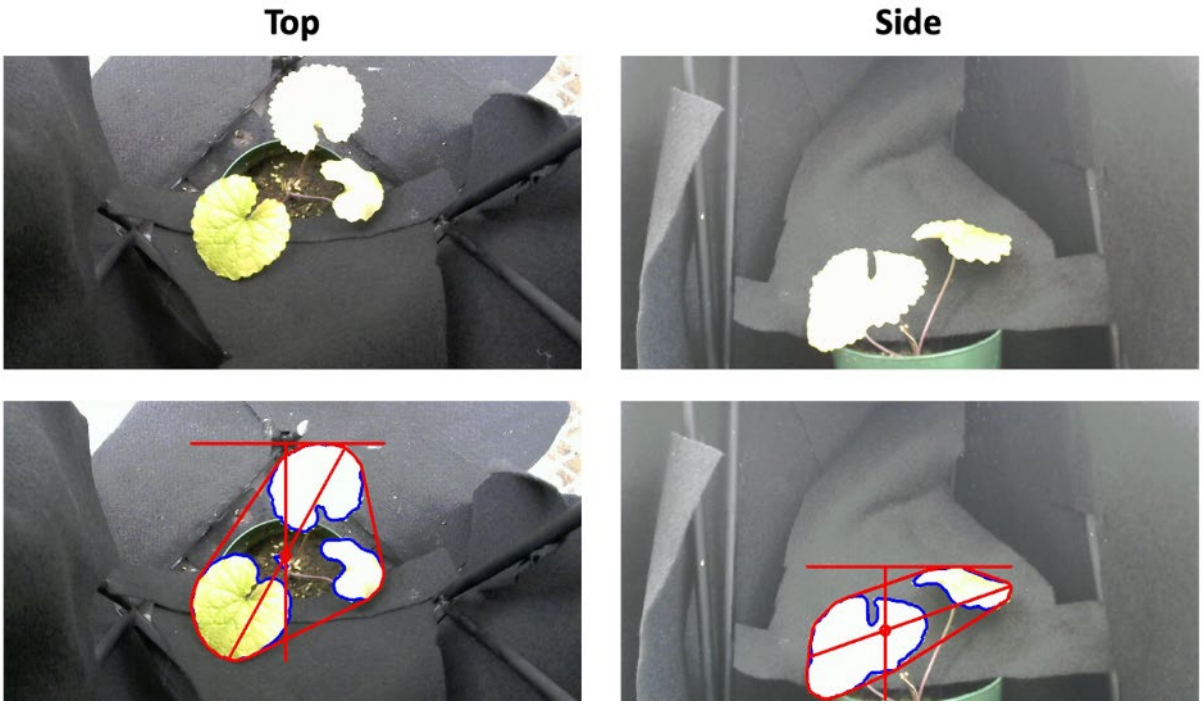

Figure A5. Example of plant identification with machine learning used to determine growth rate.

Appendix B (Supporting Information)

Table B1. Principal component loadings of *Acer saccharum* transplant size.

Principal Component	Loadings						Proportion of variance
	Stem Height (initial)	Largest leaf length (initial)	Number of Leaves (initial)	Stem Height (year 1)	Number of Leaves (year 1)	Total leaf area (year 1)	
PC1 (Transplant size)	0.45	0.40	0.26	0.53	0.25	0.48	0.41
PC2	0.42	0.09	-0.02	0.32	-0.7	-0.47	0.23
PC3	-0.18	0.62	-0.68	-0.1	-0.23	0.26	0.17
PC4	0.37	-0.49	-0.69	0.26	0.31	-0.02	0.13
PC5	0.65	0.18	0.17	-0.72	0.14	-0.07	0.04
PC6	-0.11	0.43	-0.04	0.18	0.54	0.69	0.02

Table B2. Principal component loadings of *Alliaria petiolata* transplant size.

Principal Component	Loadings		Proportion of variance
	Largest Leaf Length	Number of Leaves	
PC1 (Transplant size)	0.71	0.71	0.74
PC2	0.71	–0.71	0.26

105 **Table B3.** Summary statistics of *Alliaria petiolata* characteristics for each of the three

106 competition treatments.

Characteristic	Alone	Interspecific	Intraspecific
Greenhouse mortality	1.76% (3/170)	1.20% (2/167)	3.74% (7/187)
Field mortality	65.27% (109/167)	73.62% (120/163)	68.18% (120/176)
Relative growth rate	$1.07\times10^{-6} \pm 0.06\times10^{-6}$	1.01 ± 0.07	0.70 ± 0.05
TLA (cm^2)	9563 ± 474	8547 ± 499	5120 ± 384
Fecundity (g)	3.13 ± 0.84	1.78 ± 0.83	1.07 ± 0.38
Glucosinolate (mg/mL)	0.22 ± 0.01	0.18 ± 0.01	0.20 ± 0.01
Chl *a* (µg/mL)	0.39 ± 0.02	0.30 ± 0.02	0.34 ± 0.03
PC1 (total metabolite production)	0.47 ± 0.19	–0.43 ± 0.21	–0.05 ± 0.26
PC2 (relative glucosinolate production)	0.01 ± 0.10	–0.01± 0.10	0.00 ± 0.11
Leaf area of sampled leaf (cm^2)	3235 ± 167	3194 ± 160	2141 ± 123
Xanthomonas campestris (N)	1.60 ± 0.55	1.08 ± 0.41	1.64 ± 0.66
Thysanoptera (N)	2.87 ± 0.61	2.82 ± 0.63	4.38 ± 1.49
Erysiphe cruciferarum	35.10% (53/151)	20.80% (31/149)	26.80% (41/153)
Fern(N)	0.56 ± 0.33	1.18 ± 0.51	0.65 ± 0.50
Lifetime fitness	1.03 ± 0.35	0.40 ± 0.21	0.32 ± 0.13

107 Data in brackets denote the fraction used to calculate the percent. Plus or minus (±) values

108 denote Wald's 95% confident interval (CI) around the mean in each treatment.

109

110 **Table B4.** Principal component loadings of *Alliaria petiolata* total metabolite production and

111 relative glucosinolate investment.

Principal Component	Loadings		Proportion of variance
	Chl *a*	Glucosinolate	
PC1 (Total metabolite production)	0.71	0.70	0.84
PC2 (Relative glucosinolate investment)	–0.70	0.71	0.16

112

113

Table B5. Percent of total trait variation in *Alliaria petiolata* predicted by family, treatment and family-by-treatment interactions after controlling for transplant size. Table demonstrates the effect of including transplant size as a covariate. Only variables where transplant size was a significant covariate are shown.

Variables	**Family**	**Treatment**	**Family × Treatment**
	% (χ^2, p)	% (χ^2, p)	% (χ^2, p)
Relative growth rate	1.89 (3.2, 0.07)	**11.19 (48.9, < 0.001)**	3.22 (1.3, 0.25)
Relative growth rate†	1.16 (1.3, 026)	**13.74 (60.1, < 0.001)**	1.68 (0.4, 0.53)
TLA	0.17 (0.9, 0.35)	**27.40 (141.0, < 0.001)**	2.85 (1.8, 0.19)
TLA †	< 0.1 (0, 1)	**28.71 (149.0, < 0.001)**	2.15 (1.5, 0.22)
Fecundity*	< 0.1 (0, 1)	**11.52 (12.0, < 0.001)**	< 0.1 (0, 1)
Fecundity*†	1.08 (0.2, 0.66)	**13.20 (14.56, < 0.001)**	2.19 (0.1, 0.83)

Significant estimates ($p < 0.05$) are bolded.

* Measured on log scale

† Transplant size included

Table B6. Significance of traits on two performance metrics of *Acer saccharum* (total leaf area in year 1 and shoot mass in year 2), based on likelihood ratio tests. Separate models are performed for treatment effects (i.e. interspecific vs alone) or competitor effects (i.e. interspecific vs treatment).

Trait	**Total leaf area (Year 1)**	**Shoot mass (Year 2)**	**Data in model**
	(χ^2, p)	(χ^2, p)	
Treatment	**(17.5, < 0.001)**	**(17.6, < 0.001)**	Interspecific and alone
Transplant size	**(150.9, < 0.001)**	**(52.3, < 0.001)**	``
Leaf damage	**(24.1, < 0.001)**	(0.1, 0.8)	``
Fern	**(6.2, < 0.05)**	(0.1, 0.73)	``
Greenhouse bench*	(0, 1)	(0, 1)	``
PC1†	**(11.5, < 0.001)**	(0.4, 0.51)	Interspecific only
PC2†	**(5.8, < 0.05)**	(0.7, 0.41)	``
Relative growth rate†	(0, 0.99)	(0, 1)	``
TLA†	(0, 0.89)	**(11.5, < 0.001)**	``
Family†	(20.3, 0.57)	(26.5, 0.23)	``
Transplant size	**(102, < 0.001)**	**(40.9, < 0.001)**	``
Leaf Damage	**(12.5, < 0.001)**	(0, 0.89)	``
Fern	(1.5, 0.22)	(0.3, 0.61)	``
Greenhouse bench*	(0.3, 0.57)	(0, 0.84)	``
Field Column*	NA	(0, 1)	``
Field Row*	NA	**(4.6, < 0.05)**	``

Significant estimates ($p < 0.05$) are in bold.

* Random effect

† Competitor trait

142 **Table B7.** Significance of the effects of *Alliaria petiolata* traits on four different performance

143 metrics (TLA_{AP}, survival, fecundity, and lifetime fitness), based on likelihood ratio tests.

Competitor/Pathogen trait	**TLA**	**Survival**	**Fecundity**	**Lifetime fitness**
	(χ^2, p)	(χ^2, p)	(χ^2, p)	(χ^2, p)
Treatment × PC1	**(11.3, < 0.01)**	**(7.2, < 0.05)**	(1.1, 0.57)	(4.4, 0.11)
Treatment × PC2	(1.1, 0.57)	(1.8, 0.4)	(2, 0.37)	(0.9, 0.65)
Treatment	NA	NA	**(28.5, < 0.001)**	**(17.9, < 0.001)**
PC1	NA	NA	**(4.9, < 0.05)**	(1.6, 0.2)
PC2	(0.4, 0.52)	(2.1, 0.15)	(0.9, 0.35)	(1.2, 0.27)
Transplant size	**(11.7, < 0.001)**	(0.4, 0.55)	**(11.8, < 0.001)**	(1, 0.31)
Relative growth rate	(0, 0.99)	(0, 1)	(0, 1)	(0, 1)
TLA	NA	(2.3, 0.13)	(0.6, 0.45)	(1.6, 0.21)
Bolt size	NA	NA	NA	NA
Fern	**(5.4, < 0.05)**	**(15.6, < 0.001)**	(0, 0.84)	**(6.7, < 0.01)**
Thrip damage	(0.8, 0.37)	(0.3, 0.62)	(0.9, 0.35)	(0.2, 0.66)
Xanthomonas campestris	**(20.6, < 0.001)**	(0, 0.95)	(0.2, 0.68)	(0.3, 0.57)
Erysiphe cruciferarum	(1.0, 0.31)	(0.1, 0.72)	(0.8, 0.36)	(0.7, 0.41)
Greenhouse bench*	**(38.8, < 0.001)**	(0, 0.89)	(0, 1)	(0, 1)
Field column*	NA	(0, 1)	(0, 1)	(0, 1)
Field row*	NA	**(7.8, < 0.01)**	(0.3, 0.56)	**(5.0, < 0.05)**
Family*	(0.2, 0.69)	**(13.3, < 0.001)**	(0.4, 0.54)	**(14.8, < 0.001)**

144 Significant estimates ($p < 0.05$) are in bold.

145 * Random effect

146

147

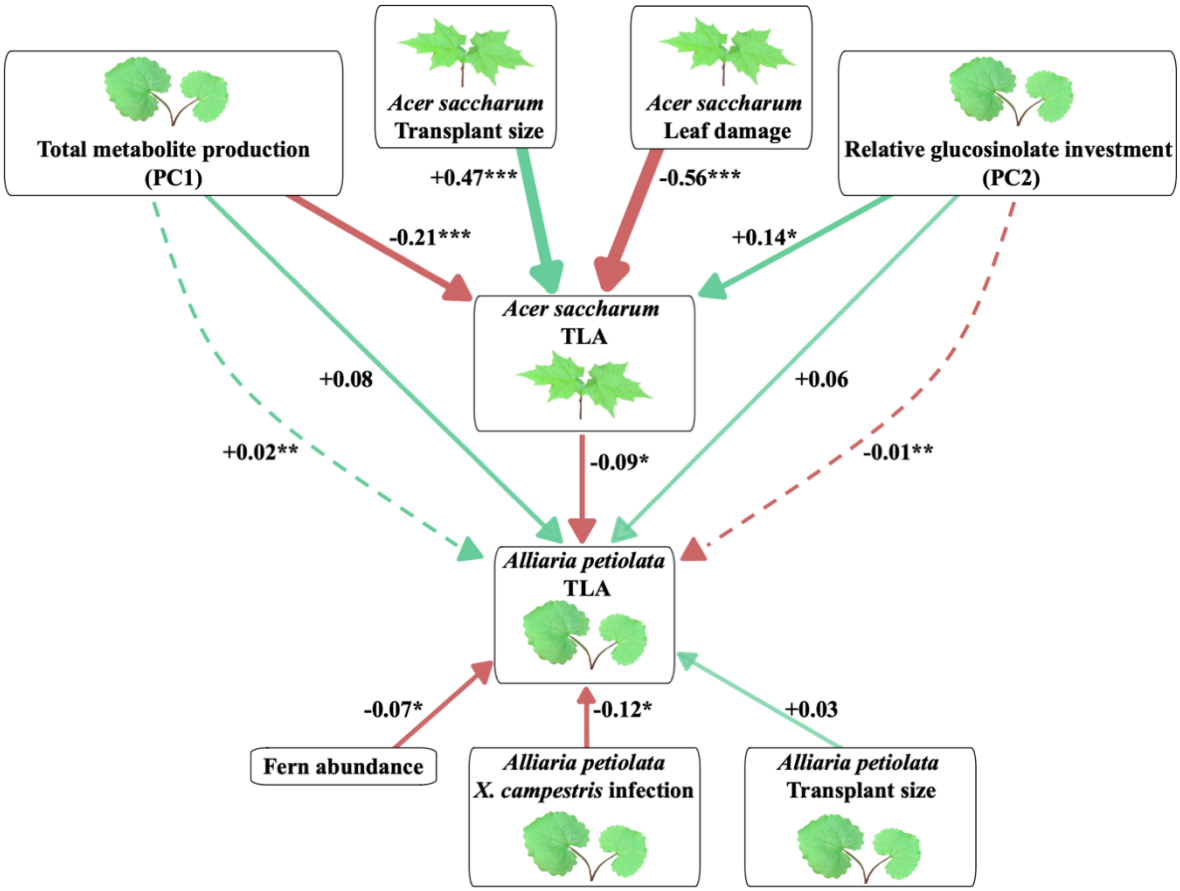

Figure B1. Path analysis of *Alliaria petiolata* total leaf area (TLA). TLA was mean-standardized while other variables were z-standardized such that coefficients represent selection gradients. Arrows denote the direction of the effect, with green arrows indicating a positive gradient and red arrows indicate a negative gradient. Arrow thickness denotes the magnitude of the effect and darker arrows indicate greater significance. The text next to each arrow shows the path coefficient and its significance level ($p < 0.05$*, $p < 0.01$**, $p < 0.001$***). Total metabolite production (PC1) denotes the production of both glucosinolates and Chl *a*, while relative glucosinolate investment (PC2) indicates the production of glucosinolates relative to Chl *a*. *Acer saccharum* TLA denotes the total leaf area of *Acer saccharum* at the end of year 1. Solid arrows represent direct effects while dashed arrows represent indirect effects.

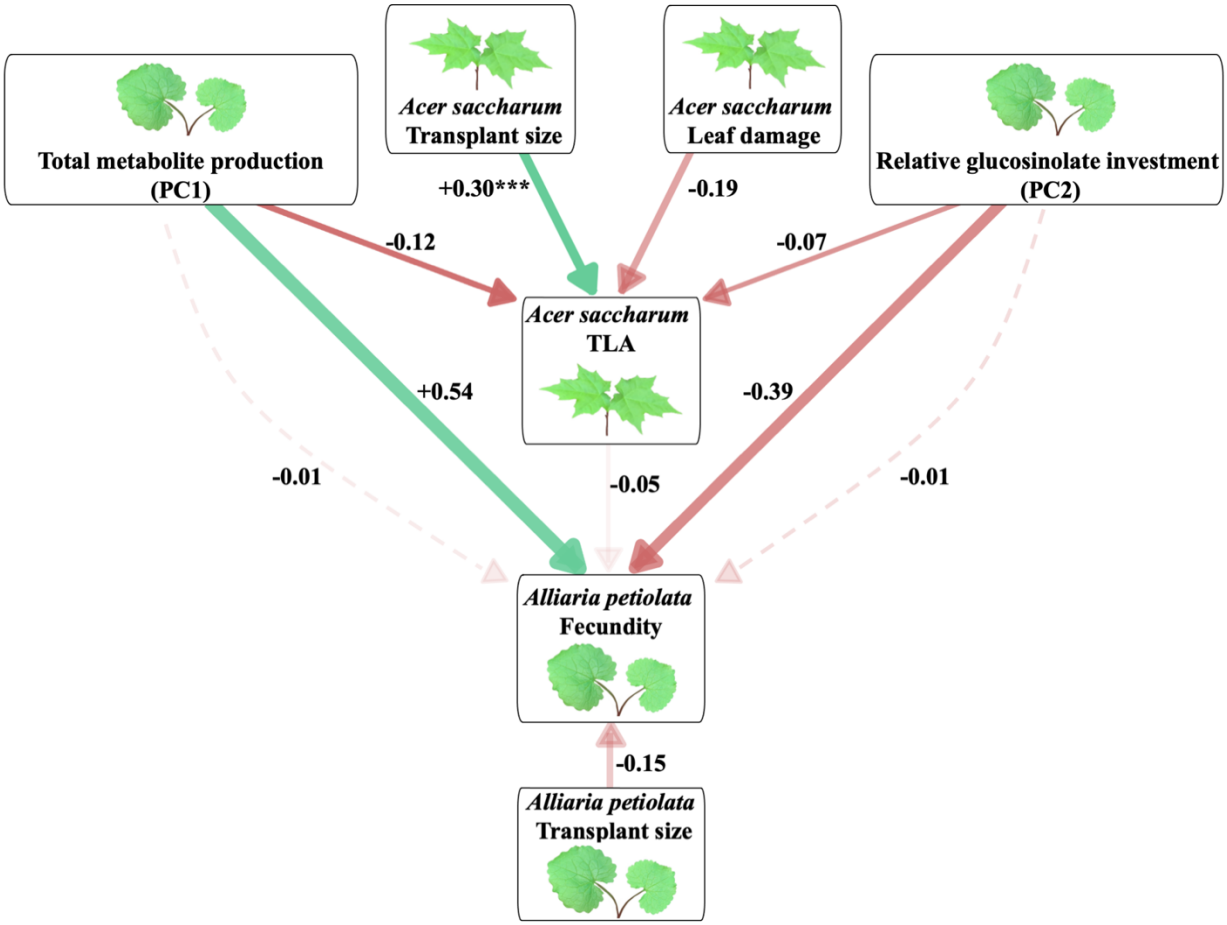

Figure B2. Path analysis of *Alliaria petiolata* fecundity. Fecundity was mean-standardized while other variables were z-standardized such that coefficients represent selection gradients. Arrows denote the direction of the effect, with green arrows indicating a positive gradient and red arrows indicate a negative gradient. Arrow thickness denotes the magnitude of the effect and darker arrows indicate greater significance. The text next to each arrow shows the path coefficient and its significance level ($p < 0.05$*, $p < 0.01$**, $p < 0.001$***). Total metabolite production (PC1) denotes the production of both glucosinolates and Chl *a*, while relative glucosinolate investment (PC2) indicates the production of glucosinolates relative to Chl *a*. *Acer saccharum* TLA denotes the total leaf area of *Acer saccharum* at the end of year 1. Solid arrows represent direct effects while dashed arrows represent indirect effects.